SATELLITE-TRACKING AND EARTH-DYNAMICS RESEARCH PROGRAMS

Grant Number NGR 09-015-002

Semiannual Progress Report No. 31

1 July to 31 December 1974

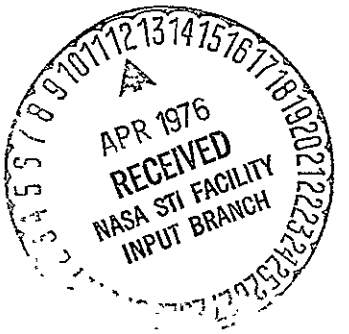

Project Director: Dr. G. C. Weiffenbach

(NASA-CR-146811) SATELLITE-TRACKING AND EARTH-DYNAMICS RESEARCH PROGRAMS Semiannual Progress Report, 1 Jul. - 31 Dec. 1974 (Smithsonian Astrophysical Observatory) 70 p HC $4.50 CSCL 22C G3/17

N76-21254

Unclas 24625

Prepared for

National Aeronautics and Space Administration
Washington, D.C. 20546

Smithsonian Institution
Astrophysical Observatory
Cambridge, Massachusetts 02138

The Smithsonian Astrophysical Observatory
and the Harvard College Observatory
are members of the
Center for Astrophysics

SATELLITE-TRACKING AND EARTH-DYNAMICS RESEARCH PROGRAMS

Grant Number NGR 09-015-002

Semiannual Progress Report No. 31

1 July to 31 December 1974

Project Director: Dr. G. C. Weiffenbach

Prepared for

National Aeronautics and Space Administration
Washington, D.C. 20546

Smithsonian Institution
Astrophysical Observatory
Cambridge, Massachusetts 02138

The Smithsonian Astrophysical Observatory
and the Harvard College Observatory
are members of the
Center for Astrophysics

TABLE OF CONTENTS

TABLE OF CONTENTS (Cont.)

SATELLITE-TRACKING AND EARTH-DYNAMICS RESEARCH PROGRAMS

Semiannual Progress Report No. 31

1. INTRODUCTION

This report describes the activities and progress during the second half of calendar year 1974. It is divided into four sections, this introduction including some of the highlights of the period. Section 2 is devoted to satellite-tracking network operations. Section 3 covers satellite geodesy and geophysics programs, while atmospheric research is described in Section 4.

A major thrust in the satellite-tracking area has been in improving the accuracy of laser ranging. Coupled with this is progress toward automated, field-generated predictions, which will both increase the amount of data and effect cost savings through reduced communications and computer usage. We are continuing to make headway in both these areas.

During the reporting period, the Smithsonian Astrophysical Observatory (SAO) network of observing stations obtained over 47,000 laser returns from the Geos 1, Geos 2, and BE-C satellites, a 48% increase over the previous 6-month period.

The upgrading of the SAO laser systems continues, with the prototype pulse-detection system already installed at Mt. Hopkins. Data are being received routinely and are being analyzed to develop new calibration procedures. The first production system, now being tested, is scheduled for installation at Mt. Hopkins in February. Fabrication of the hardware to increase the laser pulse-repetition rate from 4 to 8 pulses per minute at Mt. Hopkins has been completed, with installation planned for January.

Three of the field minicomputers are en route to their destinations in Arizona, Brazil, and Peru. They are scheduled to be operational at these sites in January, February, and March, respectively.

Design specifications have been completed for a pulse-chopping modification to the SAO laser system to alleviate the wavefront distortion problem and to increase range accuracy. A contract for the manufacture of this modification should be placed in early calendar year 1975.

A computerized geophysical data base is being designed and constructed. The first task, to develop an appropriate data-file structure and a system for managing the data, has been completed. We are beginning now to collect and compile the data.

A simulation to study network geometry is in operational status. Such a study will be important in determining the fundamental sites for the Earth and Ocean Physics Applications Program (EOPAP), under the sponsorship of the National Aeronautics and Space Administration (NASA).

A new set of 550-km X 550-km block mean gravity anomalies has been generated from 1° X 1° mean free-air anomalies. With this set plus a block estimate procedure, we now have estimates for 1452 out of a possible 1654 block gravity anomalies.

The semianalytical theory for computing perturbations on earth satellites due to direct solar radiation pressure has been documented and tested with numerical integration of equations of motion. Work is continuing on improving the perturbation theory for close-earth satellites from radiation diffusely reflected from the earth.

Preliminary analyses on ESRO 4 mass-spectrometer data have continued. A study of selected magnetically perturbed periods at 280 km clearly shows that the character of the atmospheric perturbation at low latitudes is radically different from that at high latitudes.

2. SATELLITE-TRACKING NETWORK OPERATIONS

2.1 Satellite Observing Campaigns

SAO continued to track Geos 1, Geos 2, and BE-C to provide data for its on-going research program in geophysics supported by NASA Grant NGR 09-015-002. Data acquired on these and other satellites are continually being analyzed by SAO's Analytical Satellite Geophysics Department to measure the motion of the earth's pole (Chandler wobble) and to refine geodetic parameters in preparation for future geophysical programs. These, and data subsequently acquired by the network, will form the basis for Smithsonian Standard Earth IV (SE IV), a yet more accurate model of the recently published 1973 Smithsonian Standard Earth (III) (SE III) (Gaposchkin, 1973a). SE IV is expected to provide the latest gravity-field model for the Starlette, Geos C, and Lageos satellites.

2.2 Laser Data

During the reporting period, the SAO laser stations in Arizona, Brazil, Peru, and South Africa acquired approximately 47,232 range measurements on 1873 passes of Geos 1 and 2 and BE-C (see Table 1). This total, representing a 48% increase over the previous 6 months, was achieved with a 6-day-per-week operating schedule, in spite of the fact that special testing of a new pulse-detection system was carried out at Mt. Hopkins through much of that time.

The Tokyo Astronomical Observatory (TAO) acquired 130 data points on 12 passes on its laser system during the months of August (though severely hampered by poor weather) and December. The laser system in Dionysos, Greece, owned by our cooperating agency, the National Technical University (NTU) of Athens, recommenced routine operations in July, taking 1061 data points on 209 satellite arcs. The Centre National d'Etudes Spatiales (CNES) laser system at Debre Zeit, Ethiopia, awaits return shipment to France.

Table 1. Successful laser measurements (numbers in parentheses are successful arcs).

Month	South Africa	Peru	Brazil	Mt. Hopkins	Total SAO
July	1997 (63)	5688 (198)	696 (38)	61 (3)	8442 (302)
August	1572 (60)	4408 (156)	1441 (84)		7421 (300)
September	1191 (46)	4713 (158)	1289 (70)	190 (8)	7383 (282)
October	1627 (58)	4219 (145)	2194 (95)	502 (24)	8542 (322)
November	1171 (44)	3210 (130)	1921 (106)	442 (27)	6744 (307)
December	1828 (62)	3009 (113)	1584 (91)	2279 (94)	8700 (360)
Total	9386 (333)	25247 (900)	9125 (484)	3474 (156)	47232 (1873)

Cooperating Stations

Japan	130 (12)
Greece	1061 (209)

2.3 Baker-Nunn Cameras

Ten Baker-Nunn cameras operated by SAO and its cooperating agencies obtained nearly 6000 successful observations of 16 satellites (see Table 2). These routine observations are used primarily to generate pointing predictions for the laser systems. In addition, the Baker-Nunn network supplied 2003 successful observations of five atmospheric satellites in support of NASA-sponsored research conducted by Dr. L. G. Jacchia (see Table 3).

Tracking support continued on satellite 1971 54A for Dr. D. King-Hele of the British Royal Aircraft Establishment for his study of 15th-order resonance. During a visit to SAO in October 1974, King-Hele asked SAO to continue tracking support for at least the next several months because this object is taking longer to pass through resonance than had been anticipated. In addition, special tracking support on satellites 1972 72A (Cosmos 520), 1974 17A (Cosmos 637), and 1974 60A (Molniya 51) was provided for the U.S. Air Force.

The Baker-Nunn network has established a good orbit for the Navigational Technology Satellite (NTS-1), formerly called Timation III; however, the satellite was not stabilized during this report period, and no laser ranging could be attempted.

In October, the network provided photographic support to the astronomical community during a flare-star observation campaign organized by Center for Astrophysics staff. In conjunction with optical instruments around the world, the SAO cameras photographed the flare star Y2 Canis Minoris simultaneously with x-ray observations made by the Astronomical Netherlands Satellite. The data are currently being reduced.

The Baker-Nunn camera in Australia remains in storage, awaiting construction of a new facility in Orroral Valley. SAO has proposed to move its laser system from Olifantsfontein, South Africa, to Orroral Valley in FY 1976 (see Section 2.10). The current plan is to house the laser and camera in close proximity.

Table 2. Total number of Baker-Nunn observations (by month).

Month	Number of observations
July	813
August	827
September	836
October	1291
November	1171
December	991
Total	5929

Table 3. Successful observations on atmospheric satellites (by month).

Satellite	July	Aug.	Sept.	Oct.	Nov.	Dec.	Total
Vanguard 2	55	42	55	56	51	78	337
Explorer 8	60	13	51	43	74	63	304
Explorer 19	102	108	120	149	95	35	609
Explorer 32	52	9	57	22	31	27	198
Explorer 39	131	84	107	12	83	138	555
Total	400	256	390	282	334	341	2003

2.4 Laser-Upgrading Program

2.4.1 Pulse-processing system

The prototype version of the pulse-processing system has been installed and tested and is now in routine operation at Mt. Hopkins. Personnel from Cambridge spent about 8 weeks on site checking out this first system, training station personnel, and developing field calibration techniques. The several small changes in system layout suggested during checkout to enhance operations have been incorporated into the production systems.

During checkout, we discovered that the calibration procedures for the LeCroy waveform digitizer were too tedious for a field environment. Sampling channel amplitudes and spacings could not be checked in a straightforward manner. Special calibration equipment loaned to us by the manufacturer solved the problem quite easily. This equipment has now been ordered for all the laser field stations, with delivery expected in February 1975.

Some difficulty was encountered initially with the Nanofast time-interval counter. The first unit was sent back to the manufacturer for repair, and a replacement unit was sent from Cambridge.

The new pulse-processing system requires far more extensive calibration procedures than did the old ranging system. Start-circuit calibrations, detailed target calibrations, prepass and postpass target calibrations, and special electronic equipment tests are now carried out regularly.

Even in its preliminary stages, the prototype pulse processor produced some very impressive results. Short target-calibration runs (10 pulses at fixed energy level) taken before and after satellite passes showed the system to have a root-mean-square stability of better than 15 cm over a satellite pass (see Table 4). These results were determined from preliminary calibration algorithms and during a period when calibration techniques were still being refined.

System calibration on the target has also proved to be stable and reproducible over a wide range of return signal strengths. Detailed target cali-

Table 4. Calibration stability (change between prepass and postpass calibration; preliminary).

Date	Δcal (nsec)
21 December (4)*	-0.78
21 December (7)	-0.57
22 December (0)	-1.44
22 December (3)	-0.73
22 December (5)	0.45
22 December (9)	-1.51
22 December (10)	-0.13
22 December (11)	1.16
22 December (12)	-0.26
23 December (0)	0.49
23 December (2)	-0.17
23 December (4)	1.30
23 December (6)	-0.28
23 December (8)	-0.01
24 December (3)	-0.58
24 December (9)	1.75
24 December (11)	0.55
24 December (12)	-0.53
24 December (13)	2.15
27 December (3)	-0.75
27 December (5)	1.23
27 December (7)	0.02
27 December (9)	0.70
27 December (12)	0.91

* Numbers in parentheses are hours UT.

brations as a function of signal strength taken at least once each operating night during the month of December (29 nights) have been used to determine a system calibration function and to evaluate stability. The results are shown in Figure 1. The error bars represent the 1 σ variation of the nightly averages during this period. The curve that has been fitted through the data is a preliminary version of our calibration characteristic. The data indicate that some features in the vicinity of 10 photoelectrons may not have been accounted for in our present model; however, data scatter is a bit high in this region owing to the low numbers of photoelectrons. We will examine the January data in the same manner to see if the features are still evident.

The new pulse-processing system has decreased range bias errors as a function of signal strength by almost an order of magnitude. Using both the new and the old detection systems simultaneously, with their appropriate calibration techniques, we took calibration data on the target as a function of signal strength (10 points at each signal strength). Table 5 shows the results for several nights in November. With the new pulse-processing system, the range discrepancies are mostly below 10 cm and appear to be randomly distributed in sign. The results from the old system show biases of as much as 1.5 m; they vary systematically, decreasing with increasing signal strength in all cases.

The ability of the new pulse-processing system to overcome range bias errors inherent in the old system is very apparent from satellite range data. Data taken simultaneously with the two systems have been compared by using short-arc analysis. Figures 2 through 6 show the range bias (original system minus new system) for several satellite passes. The old system, which had no means of accounting for variations in pulse size and shape, shows excursions of as much as several meters in some cases, and residual signatures with excursions of 50 cm to 1 m are common. It should be noted that these signatures have the same form as those we would expect from errors in timing, station position, and gravity field. We can expect, therefore, that these errors will systematically corrupt our measurements of these properties.

Fabrication of the data intercouplers and patch panels for the four production systems has been completed, including the modifications suggested from

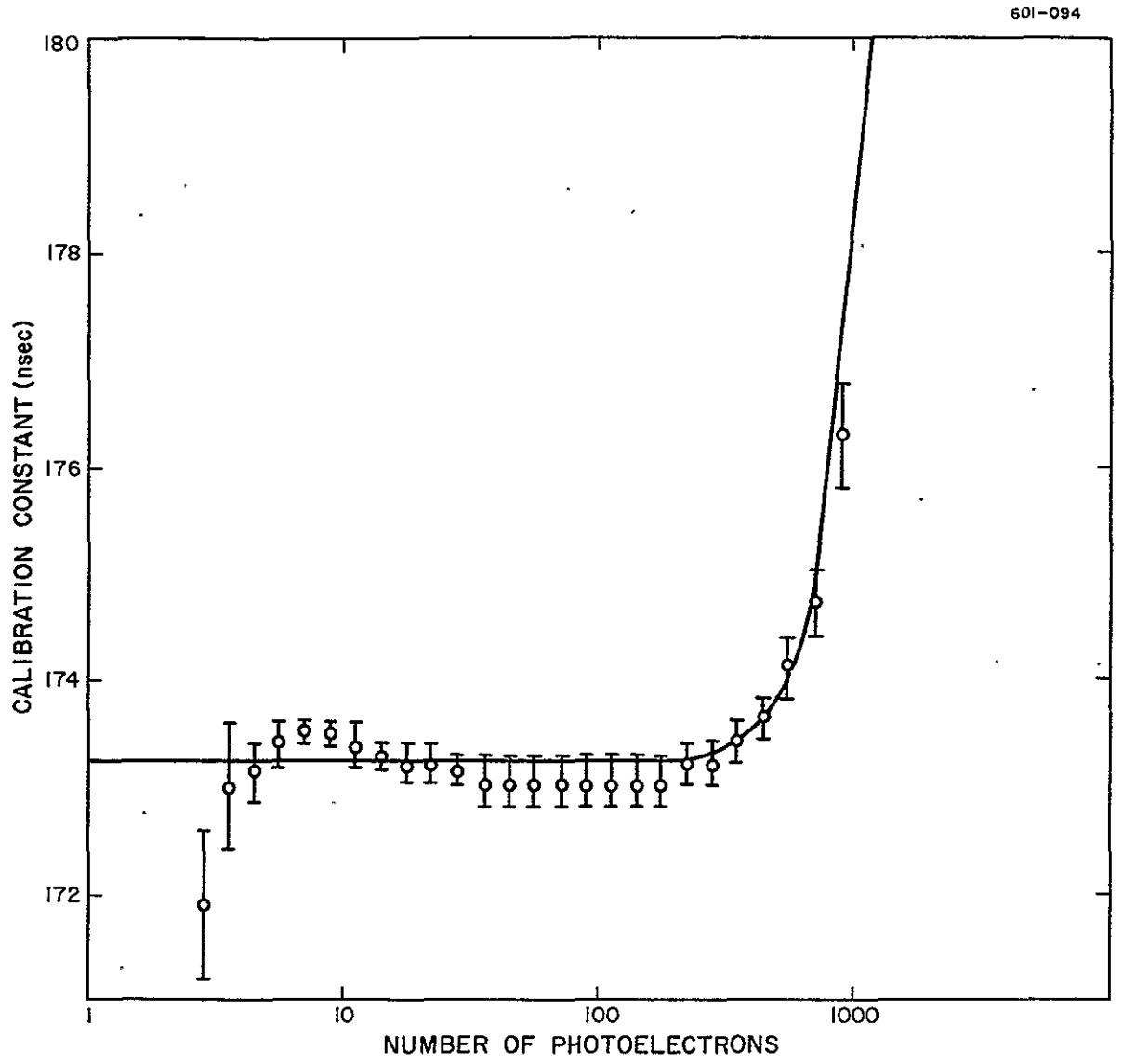

Figure 1. System-calibration constant as a function of received signal strength taken between 1 and 31 December 1974.

Table 5. Calibration comparisons, bias errors (cm).

Signal strength (photoelectrons)	18 Nov.	19 Nov.	22 Nov.	25 Nov.	27 Nov.	28 Nov.	30 Nov.
			Original				
3	170	140	—	—	—	—	87
10	60	73	142	134	40	28	4
30	—	-17	40	114	19	79	57
100	30	-15	43	7	-11	52	61
300	- 23	-60	- 4	- 11	-54	-63	- 66
1000	-140	-21	-130	-115	-71	-35	-112
			New System				
3	-14.3	19.5	-2.9	-19.1	0.9	- 5.7	-11.6
10	1.1	-21.1	—	- 4.1	2.3	—	- 4.3
30	6.9	-17.2	5.0	17.1	- 7.5	11.8	8.6
100	- 3.3	5.6	6.0	- 3.0	-11.4	-11.6	9.8
300	3.0	- 2.2	-6.1	1.0	16.8	10.4	- 2.4
1000	- 0.0	- 2.3	-0.3	- 0.7	-20.8	- 1.9	- 1.7

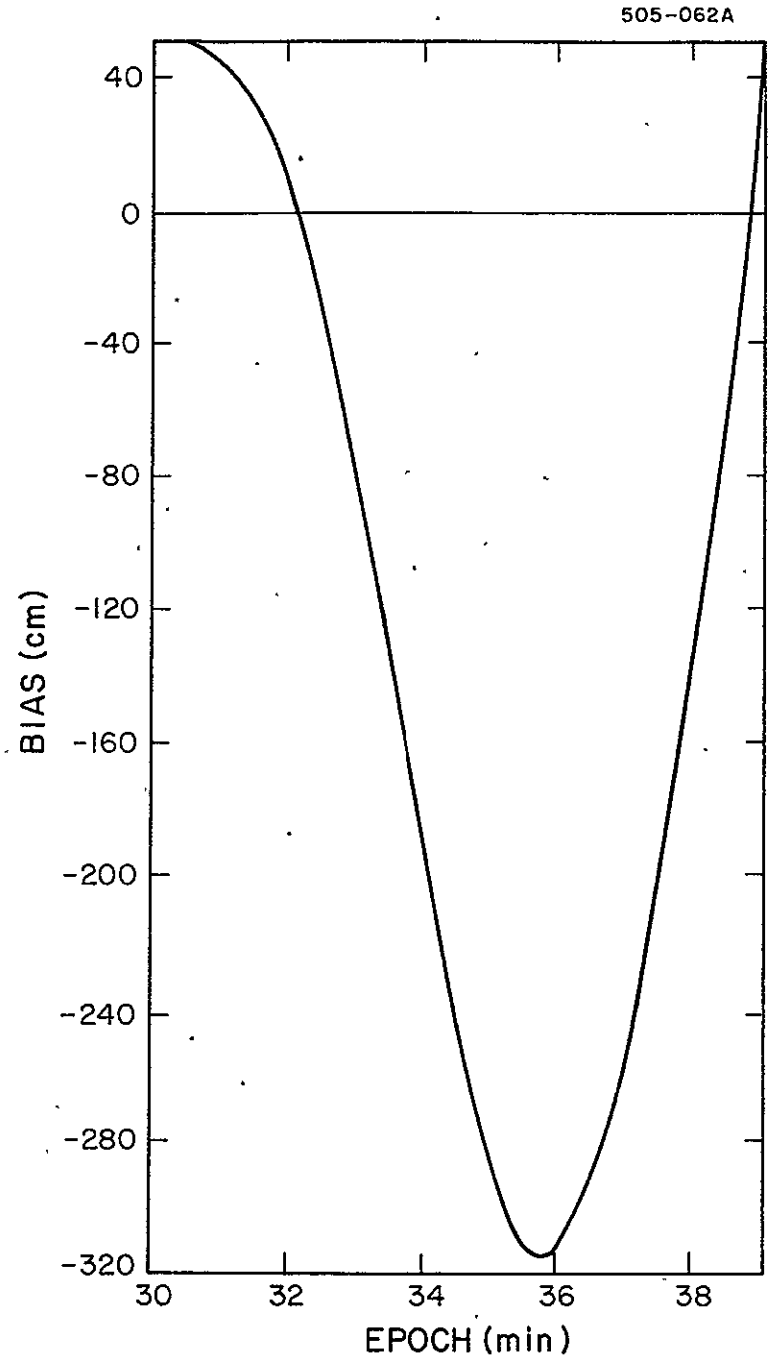

Figure 2. Range bias (original system minus new system) from the transit of Geos 1 on 30 November 1974 at 3^h30^m.

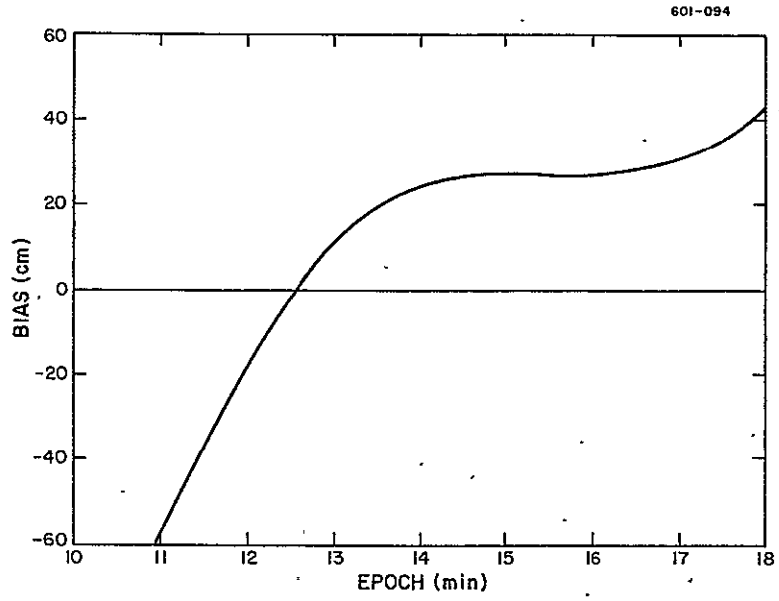

Figure 3. Range bias (original system minus new system) from the transit of BE-C on 30 November 1974 at 11^h10^m.

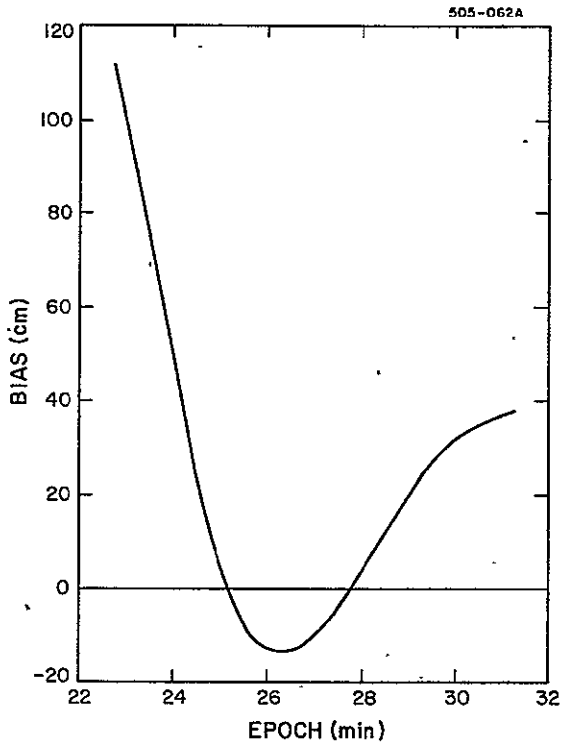

Figure 4. Range bias (old system minus new system) from the transit of BE-C on 8 December 1974 at 11^h22^m.

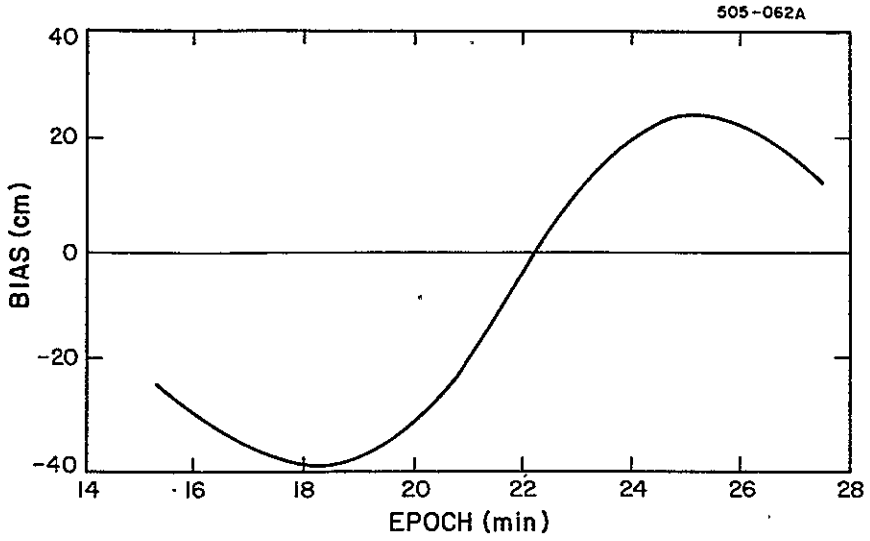

Figure 5. Range bias (old system minus new system) from the transit of BE-C on 11 December 1974 at 9^h15^m.

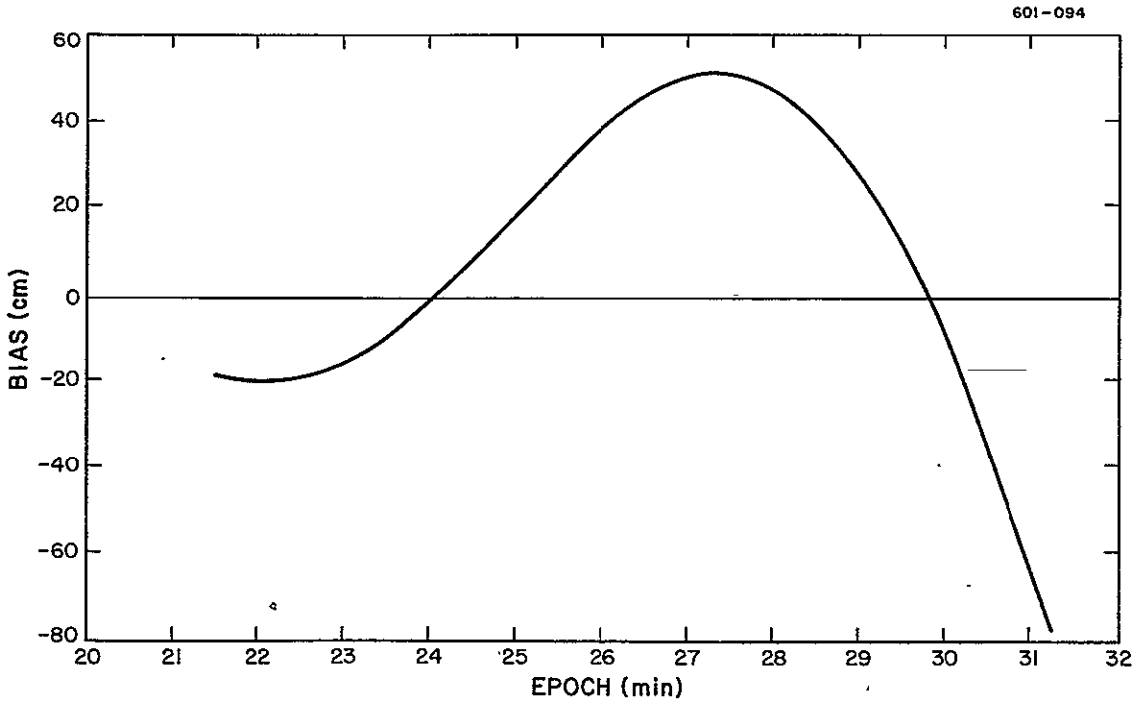

Figure 6. Range bias (old system minus new system) from the transit of BE-C on 15 December 1974 at 10^h21^m.

the Mt. Hopkins prototype fielding. The first production system is now being tested in the laboratory. We expect to install this unit at Mt. Hopkins in February and a second one in Brazil in March.

All the equipment has been delivered from the manufacturers except for the last two waveform digitizers, which are 3 months behind schedule and are expected to be delivered in February. The waveform digitizer now in Cambridge will be used to check out the third and fourth production systems; however, this will delay installation of the units in Peru and South Africa until April or May. In light of this problem, SAO is reexamining whether to postpone the installation of the fourth pulse processor until the South Africa station, which is scheduled to close on 30 June 1975, is relocated.

The first field version of the new data intercoupler manual has been completed and is in use.

Software to process the new pulse-detection system data has been developed on the CDC 6400. Programs to handle calibration and satellite-ranging data are now being used routinely with the Mt. Hopkins data. We are in the process of integrating these software packages into a production system.

Work is under way for processing the new pulse-detection system data on the minicomputer. The first task is to develop a program to handle the start-channel calibration with appropriate system diagnostics. This program is scheduled to be ready in early March.

2.4.2 Field minicomputers

Four hardware systems for on-site generation of laser satellite pointing predictions were delivered in late August. Each system consists of a Data General minicomputer with a thousand 16-bit-word memory and a floating-point processor. Attached input/output units include a teletype, a high-speed paper-tape reader and punch, an alphanumeric cathode-ray-tube display, and a three-drive Linc-tape magnetic-storage system.

Three systems have been checked out, each having a "burn-in" period of 1 month's continuous operation. The checkout period included prediction generation, diagnostic testing, and equipment operation at the line voltage and frequency utilized at the station where the unit is to be installed. In December, these systems were shipped to Brazil, Peru, and Mt. Hopkins. The fourth system awaits replacement of a malfunctioning central-processor board before it can undergo final acceptance testing. This component is due in January, and we expect to ship the system to South Africa by mid-February.

The current plan is to have all the minicomputer systems operating in the field by April, with the first one to be installed at Mt. Hopkins in January.

A prototype interface for direct connection of the minicomputer to the data system has been designed and fabricated. Testing and evaluation will be carried out at the Brazil site.

The first field version of the laser prediction program has been completed and will be checked out at Mt. Hopkins during the January installation. This program produces punched paper tape to drive the laser mount. Predictions are generated from orbital elements that will be sent through communications channels. Software for the CDC 6400 has been modified to produce orbital elements and associated information required for transmission. The program has been generating predictions in Cambridge, which have been sent out to the field for use. The program now has automatic sun- and zenith-evasion routines, as well as an initial version of an automatic power-failure/restart capability. The first field version of an operating manual for the prediction program has been completed.

Work is proceeding on the development of software to process data on the minicomputer in the field. Programs for the CDC 6400 are being rewritten to operate with the minicomputer. The first task, the rewriting of the start-channel calibration, should be completed in early March. Many of the routines will be applicable to subsequent calibration and range data-processing programs.

2.4.3 8-pulse-per-minute modification

The equipment modification to permit the Mt. Hopkins laser system to pulse eight times a minute (twice its previous rate) was completed in December. This modification will be installed in January as soon as the minicomputer is in place. The units for the other three systems will be built in January, once the modification has been given its final checkout at Mt. Hopkins.

2.5 Engineering

2.5.1 Timing

All SAO laser stations have maintained time recoverable to ±25 μsec throughout the period. Since November, SAO laser station clocks have been maintained at ±10 μsec relative to their timing reference. The Baker-Nunn stations in Spain, Greece, Hawaii, and Japan are being maintained to ±50 μsec. India and Ethiopia are currently set to WWV high-frequency timing signals owing to catastrophic clock failures.

Clock comparisons were made at Brazil, Hawaii, Mt. Hopkins, Peru, South Africa, and Spain, and the master clocks at these stations have been reset.

Rubidium frequency standards were installed as the primary oscillators in Brazil and Peru. The master clocks at all SAO laser stations are currently running from rubidium standards.

Mt. Hopkins continues to use Loran D as a timing reference. Loran C equipment has been assembled, tested, and shipped to Greece.

2.5.2 Laser systems

During the reporting period, the laser systems operated routinely, and no major problems occurred.

2.5.3 Baker-Nunn camera systems

In October, a persistent calibration-mark problem was noted at the Ethiopia station. It was traced to the EML power-amplifier system and eliminated.

The azimuth bearing in the India Baker-Nunn camera system burned out in November, a situation that has been temporarily corrected through the use of a counterweight.

Structural and cosmetic repairs were made to the physical plants of the Natal and San Fernando stations. A wheel was replaced in the rolling roof at the former site, and roof insulation was installed at the latter.

2.6 Communications

The SAO–Mt. Hopkins direct teletype system suffered some minor malfunctions as a result of extremely heavy use during testing of the pulse processor in the fall, and all the raw data had to be sent to Cambridge for analysis. The teletypes have been repaired and readjusted.

Both the ASR-28 and the ASR-32 teletype machines in Peru and Brazil were modified, the first to permit use with the laser data system and the second for use with the communications link.

The radio teletype links with Peru and Brazil operated routinely during the past 6 months. A backup LP-1007 antenna was sent to Peru and a backup Yagi to Brazil. We bought and refurbished a used ASR-28 teletype machine for Brazil as a backup for both the communications link and the laser data system.

Another used ASR-28 teletype machine was also purchased and refurbished for use with the SAO radio teletype terminal.

2.7 Data Services and Programing

2.7.1 BOLO editing

In July and August, the first version of the interactive editing package for the SAO data-preprocessing program (BOLO) was completed and demonstrated to the Data Services Division. Since this activity had been given a lower priority than the prediction and pulse-processing software, the system has not yet been put on a production basis. We expect work on this project to pick up during the next 6 months.

In December, the present version of the preprocessor was modified to handle satellite-pass data received from the new pulse-processing system in operation at Mt. Hopkins.

2.7.2 Routine operations

During this reporting period, the Data Services Division provided pointing predictions for BE-C, Geos 1, and Geos 2 for the laser sites at Mt. Hopkins, Brazil, Peru, South Africa, NTU, and TAO. Orbital elements were routinely sent to the Air Force Cambridge Research Laboratories, CNES, and the Institut für Angewandte Geodäsie in Germany for use in generating laser predictions. Camera predictions were generated and sent to 10 Baker-Nunn stations. Table 6 lists the satellites observed during this reporting period.

Orbits and predictions were supplied to the Baker-Nunn sites for satellite 1971 54A in support of King-Hele's research. NTS-1 was also observed, in preparation for laser ranging after the satellite is stabilized.

Simultaneous forecasts were provided for a campaign that used optical and laser systems in Europe and Africa on BE-C and the two Geos satellites during September through November.

Skylab predictions continued to be generated for public information.

Table 6. Satellites tracked from 1 July through 31 December 1974.

Satellite		Name
	Tracked on Request from NASA	
1963	53A	Explorer 19
1965	89A	Geos 1*
1968	2A	Geos 2*
	Tracked for Geodesy and Earth Physics	
1964	64A	BE-B
1965	32A	BE-C*
1965	89A	Geos 1
1968	2A	Geos 2
1968	109A	Peole
	Tracked for Long-Period Perturbations	
1959	$\alpha 1$	Vanguard 2
1960	$\iota 2$	Echo 1 Rocket Body
1964	64A	BE-B
1965	89A	Geos 1
	Tracked for Atmospheric Investigations	
1959	$\alpha 1$	Vanguard 2
1960	$\xi 1$	Explorer 8
1963	53A	Explorer 19
1966	44A	Explorer 32
1968	66A	Explorer 39
	Special Requests	
1971	54A	Thor Burner 2 Rocket
1972	72A	Cosmos 520
1974	17A	Cosmos 637
1974	54A	NTS-1
1974	60A	Molniya S1

*Satellites ranged by lasers during this 6-month period.

SAO laser data for FY 1974 were validated and made available to the Analytical Satellite Geophysics Department for analysis. The Data Services Division continued reevaluating data from the International Satellite Geodesy Experiment (ISAGEX) and the Earth Physics Satellite Observation Campaign (EPSOC).

The film-control section received and cataloged 5373 observations on 3452 films from the SAO Baker-Nunn sites plus 812 films from Air Force sites.

A total of 1345 satellite positions were precisely reduced, bringing the number of all reductions to 244,977 as of 31 December 1974. Of the total for this report period, 238 reductions were made by the Instituto di Geodesia, Bologna, Italy, in cooperation with SAO. Table 7 gives a breakdown of the precise reductions during this period.

2.8 Special Experiments

Special experiments on the laser wavefront distortion and the effect of water-vapor absorption on return-signal strength have been performed with support from both the Office of Tracking and Data Acquisition (OTDA) and the Office of Applications (OA). They are reported in Section 3.8.

2.9 Personnel

During this period, Messrs. Denison Rich and Dana Seaman, new-hire observers, successfully completed their training and were assigned for permanent duty in Arizona and Brazil, respectively.

Mr. D. Kirk Gilmore, a Tucson resident, was hired as a Baker-Nunn camera operator at the Mt. Hopkins station in July.

Mr. Harilaos Billiris, Boston University graduate student and former member of the Dionysos, Greece, station staff, completed his work on systems analysis of the SAO laser systems and returned to Greece in October. Billiris, whose work for a Master's thesis included quantitative data on wavefront dis-

Table 7. Reductions completed 1 July through 31 December 1974.

Object	Period	Number of images	Investigator
Explorer 19	December 1972 to April 1973	602	Jacchia
Echo 1 Echo 2 Pageos Explorer 39	September 1966 to June 1969	509*	WEST
Explorer 39	October 1968	238*	Jacchia
	Total	1345	

*Selected simultaneous observations.

tortion and demonstrated the possibility of a 30% reduction in the range-measurement error by using pulse photograph data, was originally hired for the summer and worked closely with SAO staff scientists Dr. Michael Pearlman and Mr. Carlton Lehr during his tenure at the Observatory.

Mr. C. Robert Bennett, former station manager in Olifantsfontein, South Africa, resigned as of 30 September 1974.

2.10 Special Projects

Discussions have been under way with NASA OTDA and with Messrs. Peter Morgan and Dennis Willshire of the Australian Division of National Mapping and the Australian Department of Science, respectively, concerning the proposed move of the SAO laser system from South Africa to Orroral Valley, Australia. Orroral Valley is a prime candidate for a site in view of its southern-hemisphere location, geological stability, and climate. In addition, the fact of its being an already established site offers advantages in communications and logistics. SAO had originally proposed to locate on a hilltop above the valley to take advantage of the localized meteorological and geological conditions; however, in view of the high costs involved, OTDA has recommended a site on the valley floor in proximity to the NASA facilities. Pearlman will go to Australia in January to prepare cost estimates with Willshire for presentation to NASA.

During late September and October, audits were conducted by the SAO Controller's Office staff at the Mt. Hopkins and Maui observing stations. Similar audits are planned for Brazil, Peru, South Africa, and India within the next 6 to 8 months.

3. SATELLITE GEODESY AND GEOPHYSICS PROGRAMS

3.1 Introduction

During the period 1 July to 31 December 1974, research has been directed toward studies of the dynamics of the solid earth as related to Earthquake-Hazard Assessment (EHA) models. According to objectives delineated in SAO's 10 Research and Technology Operating Plans (RTOP), divisional efforts have included improvement of satellite ephemerides; use of existing satellite-tracking data for the determination of geophysical parameters, such as the gravity field, earth tides, polar motion, and station location; reduction and analysis of geodimeter measurements to determine local movements of the earth's crust; and studies to establish requirements for satellite-tracking equipment, network distribution, and satellite design.

The scientific work related to individual RTOPs is discussed in the following subsections.

3.2 Geophysical Data Base (RTOP 369-01-04)

A computerized geophysical data base (GDB) is being designed and constructed. Our long-range goal is to computerize all available and appropriate data for the earth-dynamics areas of the Earth and Ocean Physics Applications Program. The GDB fulfills a need at SAO for a system to manage large numbers of data to be used in analysis; we are hopeful that it will become the basis for a cooperative effort of collecting and managing data of mutual interest to a larger group of scientists.

The first task, to develop an appropriate data-file structure and a system for managing the data, is finished. The result is a general data-management system that provides a random-access capability for large numbers of data. The system operates on a CDC 6400 computer using a combination of magnetic tape and disk storage.

The programing effort for the GDB has been completed. A Fortran subroutine package has been written to simplify the maintenance and use of the data. Utility programs have been prepared that allow the user to create a private data base and to deactivate a bad pool tape. Changes to the basic read routine now make it more efficient. A protection system has been added to the existing password system, enabling users to be divided into categories according to permission levels.

A bibliography file for the data base has been designed and is being implemented. The file contains one entry for each source of data included in the data base and will itself be a GDB data file. A program has been written to allow the user to add a new entry to the bibliography file, delete or change an existing entry, or look up a reference already in the file. In looking up an entry, the user can specify as little or as much information as is known about the author(s), year of publication, and GDB reference number. New entries to the bibliography file will be written in a standard format, a description of which will be distributed to those adding entries to the GDB bibliography file.

The second major task in establishing the GDB is under way: to collect and compile data. A few data are now available. We have begun to select geological and tectonic data to be incorporated and have been establishing a method to compile the data and data source and the mechanics to convert essentially graphical information (maps) into digital form.

A plot of data gathered on earth plate boundaries has been completed. In addition, data of digitized plate boundaries have been obtained from Dr. S. Solomon of Massachusetts Institute of Technology. Both sets of data are being converted from their current computer formats to forms usable by the GDB.

We have begun planning for the incorporation of geological data. Few such data are currently available in computer-accessible form, consisting mostly of maps and descriptive text.

New files being generated include a plate-boundary file incorporating Solomon's data and a combination 1° X 1° mean-gravity-anomaly file.

A program that determines the relationship between topographic heights and gravity anomalies has been written. It performs a regression analysis utilizing any 1° X 1° topographic height file and any 1° X 1° gravity-anomaly file.

A writeup and user's manual for the GDB has been prepared by Dr. M. Williamson and Ms. L. Kirschner and will be published soon.

3.3 Tectonic Plate Motion and Fault Motion (RTOP 639-02-01)

An understanding of tectonic plate motion and fault motion is necessary for the successful development of an EHA model. It is believed that plate motion is the primary source of energy for earthquakes, which are plate-boundary phenomena. Earthquakes can be studied by determining large-scale plate motion and deformation and small-scale deformation near these boundaries. Precise determination of the fundamental EOPAP station locations will provide a reference frame for measuring plate motion and deformation.

The broad objective of this RTOP is to develop a computational technique and a project plan to measure plate motion and deformation and to provide data for an EHA model. The data-acquisition and data-processing system will lead to an operational system. The main objective is to determine ground-station positions with an accuracy of ±5 cm by 1976, by using satellite laser ranging data plus other data such as from very-long-baseline interferometry, lunar laser ranging, tracking of deep-space probes, and surface measurements. The program plan will provide interstation vectors to 10 cm by FY 1976, plate motions to 10 cm $year^{-1}$ by FY 1978, and plate positions to 10 cm plus plate motions to 2 cm $year^{-1}$ by FY 1980.

The most accurate EOPAP satellite orbits will be short arcs for a week or less, determined from observations taken by the fundamental network of laser tracking stations. Tracking-station navigation will then provide precise station positions in center-of-mass coordinates. An extension of this technique can be used to calculate very precise interstation vectors, by minimizing the

observational residuals taken two at a time. Computer software will be developed and analysis will be started to determine the accuracy attainable. The completeness of the orbital theory, various kinds of errors, and selected distributions of observational data will be studied to establish the sensitivity of the station-position determination to these factors. Interstation vectors determined from these short-arc computations will be combined into a regional or global network in an adjustment computation. The network geometry and error sources discussed above will be studied by means of a simulation, which will establish the degree of sensitivity to error sources, network geometry, satellite geometry, and data volume. Other data types will also be included in both the analysis programs and the simulation.

Suitable existing tracking data will be selected for use in this analysis. The ISAGEX, EPSOC, and Geos 3 observing campaigns will provide data enabling us to verify the analysis programs and the accuracy estimates used in the simulation. A program of observations will be initiated to obtain tracking data that can measure plate motion. Selection of sites and satellites will be based on the simulation analysis, and existing facilities will be chosen if possible. Such an experiment will demonstrate the feasibility of this approach and may not be optimum for an EHA model. Finally, based on these analyses, a program plan will be developed to obtain systematic measurements of plate motion.

The simulation program is in operational status and is being used to study network geometry for fundamental sites for the EOPAP network. The error model used in the simulation program for the observations and the gravity field is quite realistic with regard to average data already processed. The assumed 1.5-m accuracy of the station coordinates is too optimistic by a factor of 2 or 3. If we take that factor into consideration, application of actual tracking data to date would show excellent agreement with the simulation error model. Orbit computation accuracy is 5 to 6 m.

During this reporting period, Mr. J. Latimer and Ms. M. Anderson began a series of runs to analyze the geometrical characteristics of single passes of Lageos, with the purpose of studying the information contained in a single

pass of this satellite. Minor modifications to the SAO orbit-determination program were made to enable one- and two-dimensional variations of station coordinates in the single-pass analysis mode. In addition, a four-station network and a six-station network were simulated, incorporating up to 36 passes, in order to determine the minimum number of passes required for optimum results.

In another simulation run using a fictitious equatorial station (approximately 0° latitude and longitude), three simulated passes of Lageos were generated with maximum elevation angles of 30°, 45°, and 60°. A random noise of 10 m was introduced as the only error, and for successively smaller arcs of each pass, the displacement of the station coordinates z, x, then z, y, and then x, y, z were determined. The same investigation was then made by assuming a range bias of 10 m as the only error.

Work has begun on the short-arc analysis of simultaneous observations. The first experimental run to analyze the geometric characteristics of single-pass error propagation for the Lageos tracking system has been completed.

Analysis of ISAGEX optical data is well under way. The laser data were reduced first and have been used in global solutions for the geopotential and station coordinates. ISAGEX data are of sufficient quality and quantity to provide a global geocentric reference frame with an uncertainty of less than 5 m. The reduction of camera data has been completed and analysis has begun. New data from a number of camera sites not used in earlier solutions now augment the data.

The analysis has been carried out in three different ways: 1) a geometrical determination of the network, 2) a dynamical determination of station coordinates, and 3) a combination of the two sets of normal equations. Preliminary results of these three solutions for four satellites and five stations participating in ISAGEX were reported at the INTERCOSMOS Symposium on Results of Satellite Observations in Budapest in October (Gaposchkin, Latimer, and Mendes, 1974). Two of the stations — Riga and Zvenigorod — show good

agreement with earlier solutions; the other three — Ypburg, Potsdam, and Cairo — are completely new to the SE III reference system. Other conclusions from the paper follow:

A. The optical data taken during ISAGEX are compatible with other data and have an accuracy of 3 to 5 arcsec as determined from both geometrical and dynamical analyses.

B. The optical data taken in ISAGEX have been successfully combined with other data in a determination of station coordinates.

C. Further analysis is indicated. More data can be incorporated and coordinates of stations participating in routine observations can be determined.

D. Precision ephemerides for Pageos are difficult to determine because of radiation pressure, albedo pressure, gravity-field resonance, and the nonsphericity of the satellite. Further analysis is needed.

The orbital arcs used in the dynamical solution and the final station coordinates determined are given in Tables 8 and 9.

Further analysis is being carried out for a revision of these same five stations and possibly more.

Since the October meeting, Latimer has been reanalyzing the Eastern block ISAGEX data; a completely reprocessed geometrical solution has been obtained and a new combination solution is nearly complete. The principal features of this new analysis are a more powerful treatment of the rather abundant Pageos data by the dynamical method (by employing a more sophisticated handling of radiation pressure) and an iterative procedure of determining station timing corrections to the Eastern block data. Various improvements to the data-handling program have been made, and a documentation of the results is in progress.

We expect to be able to apply results from this work in our analysis of Lageos data, particularly in view of the improvements to the radiation-pressure model. We hope also to incorporate the Eastern block stations in the SE III reference system.

Table 8. Orbital arcs used in the dynamical solution.

Satellite	First date (MJD)	Last date (MJD)	σ_0	n	Station and number of observations 1055	1084	1181	1901	8034
6508901	41005	41014	1.88	1182	17	7	6		
6508901	41018	41026	2.32	445		31	52		
6508901	41133	41133	1.17	1154	19			7	
6508901	41152	41163	1.04	868				10	
6800201	41036	41042	1.49	426					17
6800201	41002	41048	1.86	493		9	18	8	
6800201	41054	41062	2.06	659	1	7			10
6800201	41176	41189	1.35	866				16	20
6102801	41011	41044	0.90	1708	50	20		87	
6102801	41136	41184	1.10	1048	25		9	273	
6605601	41010	41024	0.96	1042	459			11	
6605601	41024	41038	0.40	452	100	45		57	

Table 9. Final coordinates.

Station	X (Mm)	Y (Mm)	Z (Mm)
1055	3.9074101	1.6024417	4.7638993
1084	3.1838814	1.4214803	5.3227977
1181	3.8006135	0.8820000	5.0288464
1901	4.7283152	2.8796455	3.1568594
8034	3.9196373	0.2988292	5.0059135

Also to be incorporated in defining mean station coordinates are the effects of body and ocean tides, as the ability to determine such is connected with the ability to define a suitable reference system for orbit computation. Mr. A. Girnius has been studying the Love elastic parameters h and ℓ in order to compute station displacements due to linisolar tides. The parameters h and ℓ are not constants, but rather functions of the earth's radius and gravity. Girnius has been employing a simple model to compute these numbers and their combinations for each station used in SE III. According to this model, the differences for stations near the poles and the equator are small, and for the time being, we can assume them to be constant ($h = 0.637$ and $\ell = 0.090$).

3.4 Polar Motion and Earth Rotation (RTOP 369-02-02)

This task addresses itself to measuring variations in the earth's rotation and polar motion, with a long-range goal of 1-cm accuracy from data acquired over a 12-hour average and a near-range (1977) goal of 10-cm accuracy over a 24-hour period. Understanding and measuring polar motion will contribute to the EOPAP objective of obtaining an EHA model in three ways: 1) a possible earthquake-precursor signature will be derived, 2) information will be gained on the elastic and dissipative properties of the earth, and 3) pole positions will be used for more precise orbit computation.

Information on the bulk elastic and dissipative properties of the earth can be extracted from rotation measurements. Since the EOPAP observations of earth rotation will be some 2 orders of magnitude more accurate than the classical data, significant new results are expected. Earth rotation can be recovered by determining the location of ground stations with respect to suitable orbits as part of the orbit-determination computation. We are doing this with precision laser range observations, wherein mean orbital elements are derived for several months to establish a reference orbit. Polar motion, which appears as diurnal variations with respect to an orbit, is calculated by least squares.

The deterministic model for polar motion plus earth rotation will be a numerical integration of the equations of motion for a nonuniform viscoelastic rotating body that includes nonlinear core-mantle coupling.

It is known that extensive mass shifts accompany earthquakes, and it is believed that a significant part of these shifts may precede large earthquakes by several days. These mass shifts alter the moment of inertia of the earth and, therefore, the earth's rotation rate and rotation axis (pole position). It has been estimated that a change in the geographic location of the spin axis of 1 cm should accompany an earthquake of Richter magnitude 7.5. This change is measurable with Lageos and 2-cm-accuracy laser range measurements.

Preliminary results from using laser tracking data in our studies of polar motion are available. The motion of the pole is defined through the theory of precession and nutation. By choosing a period where effects of nutation are relatively constant, variations in pole position have been calculated. The agreement between pole position determined from laser satellite-tracking data and that determined by the Bureau International de l'Heure (BIH) is 1 to 2 m.

Now added to the orbit-computation program are the perturbations and satellite positions due to the elastic deformation of the earth caused by polar motion (Gaposchkin, 1973a, p. 159; for further details, see Gaposchkin, 1973b). The effects are small but can amount to 1 m, which is a very modest but detectable improvement, considering the current orbit-computation accuracy. This result hinges on the assumption that the mean pole of the earth is the same as the axis of maximum moment of inertia. In a few years, as other orbit errors are reduced, this effect will allow the axis of maximum moment of the earth's inertia to be derived from satellite-tracking data.

Laser satellite-tracking data impose scale on both the orbit and the size of the earth. Previously, the abundance and distribution of data were not sufficient to improve the value of GM of the earth as determined from deep-space probes. Now, initial tests with laser tracking data at current orbit-computation accuracies suggest that the values of both GM and scale for the earth can be improved. Preliminary results indicate that the current value of GM should be changed by approximately 1.5 parts per million and the scale of the earth by 3 times that amount.

In back of these new results is a continual process of updating UT1 polynomial coefficients and coordinates of the earth's pole position, an encom-

passing task pursued by Girnius. Geodetic coordinates of 25 international satellite observing stations have been compiled from various sources and transformed to the SAO format. In December, Girnius attended the Sixth Annual Precise Time and Time Interval Planning Meeting, sponsored by the United States Naval Observatory, at which experts in the field discussed applications of new techniques for determining the earth's crustal movements, polar motion, and rotation.

3.5 Gravity Field and Tides (RTOP 369-02-03)

An accurate gravity-field model, as required by EOPAP, is necessary in order to provide precise satellite-position information in support of satellite altimetry, magnetometry, and polar-motion and plate-motion determination. The best gravity fields for ephemeris calculation will come from analyses of satellite-tracking data. In fact, a satellite-determined gravity field is an essential boundary condition on all upper mantle and convection models, and an improved gravity field is essential for analyzing Geos 3 and Lageos data.

During this reporting period, an SAO Special Report describing a new set of of 550-km X 550-km block mean gravity anomalies generated from a more complete set of 1° X 1° mean free-air gravity anomalies was written by Williamson and Gaposchkin (1975). After obtaining and combining four sets of 1° X 1° mean anomalies from different sources, they compared the data with a previous compilation. The result is a composite set of 31,654 1° X 1° mean anomalies. Using this set and a block estimate procedure developed by Kaula (1967), Williamson and Gaposchkin have now derived estimates for 1452 out of a possible 1654 block gravity anomalies. This figure represents 88% coverage of the earth, a 22% increase over the coverage used in SE III. A map of the distribution of these 1° X 1° measured anomalies has been made (Figure 7).

The covariance function of 1° X 1° mean topographic height was also calculated, and a regression analysis of surface-gravity data and topography was performed. These have resulted in a better understanding of the dependence of

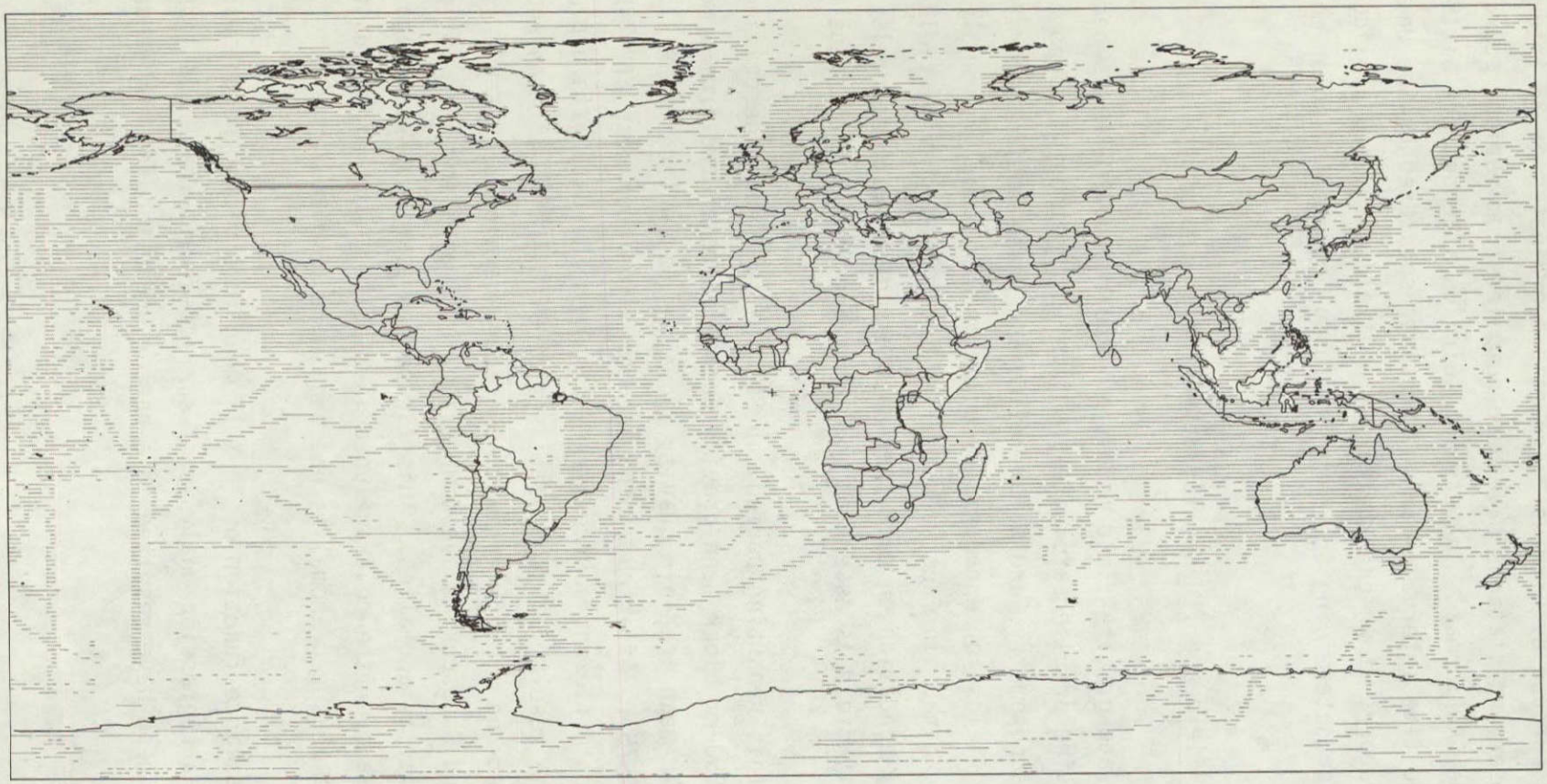

Figure 7. Distribution of 1° X 1° mean surface-gravity data.

1° X 1° surface gravity on topographic height. Comparisons indicate that the variance of terrestrial gravity data cannot be better than 15 to 20 $mgal^2$.

Higher potential gravity-field coefficients ($\ell \leq 36$) have been calculated from the new set of mean block gravity anomalies by quadrature in order to estimate the mean square error of the geopotential model. The mean potential coefficients for degrees through 36 have been plotted; the resulting geoid height shows only minor changes from SE III.

The computer program that calculates potential coefficients from surface-gravity data by quadrature has been revised to calculate mean potential harmonics, thus increasing the accuracy of the procedure. As a result, the fit of the calculated gravity field to the surface-gravity data has been improved by 10%. In addition, the variation of the mean potential coefficient by degree is closer both to theoretical predictions and to independent calculations.

Also in revision is a scientific program that calculates normal equations from the surface-gravity data to obtain the potential coefficients. The resulting program will allow a complete gravity-field solution with all potential coefficients up to degree and order 36. The accuracy of the procedure will be improved further. Previously, the capability was limited to a set of 290 coefficients.

During this reporting period, a somewhat condensed version of the 1973 Smithsonian Standard Earth (III) was published in the Journal of Geophysical Research (Gaposchkin, 1974). Gaposchkin also compiled a four-year summary of the status of satellite geodesy, to be published by the American Geophysical Union (Gaposchkin, 1975).

3.6 Ground Systems Requirements and Plans (RTOP 639-01-03)

It is now believed that the plate-tectonic hypothesis provides the best unified conceptual framework for understanding phenomena such as earthquakes, continental drift, volcanism, and mountain building. Therefore, an understanding of the fundamental mechanisms underlying earthquakes will be based on this concept. A principal objective of EOPAP is an EHA model, which depends on

satellite measurements of plate motion as well as on surface measurement of interplate and intraplate deformation and on an increased understanding of the mechanisms driving plate tectonics. Satellite determination of plate motion, in turn, depends on the positions and selection of sites used for EOPAP. Locations must be selected to avoid local phenomena that will mask the geophysical features of interest. Sites must also be chosen to ensure adequate geographical distribution and data volume, accessibility, and accuracy. Careful consideration also must be given to weather, cloud cover, logistics, and availability of support in the local political environment.

The objective of this task, therefore, is to establish the number and distribution of laser satellite-tracking stations required for the fundamental EOPAP network. The selection of sites will necessarily be one of successive trial. A set of individually acceptable sites will be tested in a computer simulation for adequacy in orbit computation; plate-motion, polar-motion, and earth-rotation determination; and data volume and completeness. Satellite-tracking lasers will then be assigned to the fundamental network in the context of all stations in the EOPAP program (for example, lunar lasers, VLBI, or lasers furnished by other countries).

In addition to a priori site selection, we are establishing the requirements for surface measurements that have to be made in the neighborhood of each fundamental site to provide assurance that our observations are not contaminated by unknown local anomalies, for example, tides, tidal loading, or local crustal movements. If necessary, a program of concurrent surface measurements will be established for each fundamental site to provide necessary information for the interpretation of satellite-determined positions and motion.

Drs. N. H. Mao and P. A. Mohr are gathering geological and geophysical information on 26 proposed fundamental tracking sites. They will be evaluating these locations in terms of local and regional stability. A preliminary version of their report has been completed, and a more extensive compilation is in progress.

At the same time, Mao has planned a project to monitor microearthquakes near fundamental stations and has written a report describing such a project. With a three-component event recorder located near a station and two vertical-component recorders at the other two vertices of a triangle, a tripartite array would be formed that could measure the regional stress field over a period of 1 or 2 years. The spatial and temporal distributions of a microearthquake will give ample indication of the stability of a station. Assuming a uniform stress near the station, a composite fault-plane solution can be obtained that will give us the regional stress field near the station. Such a system appears to be highly desirable to ensure the selection of tectonically quiet, stable locations, as evaluation of geological and geophysical data alone may not provide sufficient information.

A new three-component microseismometer is available at a cost of less than $2,000. Mao is checking into this and other commercially available or newly designed seismographs.

Procedures for determining station corrections due to elevation differences and to lateral inhomogeneities of the earth's crust and for deriving a hypocenter location for the above-mentioned tripartite array have been reviewed and documented.

3.7 Analytical Models of Earth Motion (RTOP 161-02-07)

The ultimate objective of this task is to compute the complete strain field for the earth's interior for the development of EHA models. Basic data will include gross earth data, such as the geopotential and seismic travel times, and detailed surface measurements, such as of plate motions. The large-scale deformation field will be formulated in spherical coordinates, and the solution will be obtained by numerical integration of partial-differential equations.

The EHA models will be generated by computer programs that will convert geophysical parameters and observations into predictions of probable times,

places, and magnitudes of earthquakes. Analysis of the required inputs indicates that the most difficult tasks for the preliminary model are those necessary for determining regional strain fields and global plate motions. Because the pattern of crustal movement and deformation in fault zones is directly related to the occurrence of earthquakes, such information necessarily constitutes a primary input to EHA models. At least two, and preferably more, regions should be surveyed for the preliminary EHA model in order to avoid the danger of having the overall program distorted by unique characteristics of some particular geographic region.

The deformation of the earth can be described by a system of nonlinear partial-differential equations. We will select the appropriate formulation in spherical coordinates and will include elastic, viscous, and anisotropic factors. The differential equations will be established relating the observables and the strain field. They will be integrated with numerical methods by using boundary conditions given as gross earth data and detailed surface measurements through the computer-accessible GDB.

The short-term goals for this study are 1) to develop the basic mathematical model for earth strain (including the dependence on observable parameters, 2) to study the numerical methods necessary for solving this system of partial-differential equations, 3) to develop preliminary computer programs, and 4) to establish computer requirements for a general solution that will incorporate observational data.

The basic constitutive equations governing deformation have been reviewed. The details of the interaction of plate boundaries seem to be critical for developing a realistic model. A local model is being considered to determine the horizontal scale of deformation; this model is based on two semi-infinite slabs undergoing relative horizontal motion (on the average) with a point on the interplate boundary locked.

3.8 Laser Techniques (RTOP 639-05-02)

We have continued developing and analyzing our laser systems in order to meet the increasingly stringent data requirements for EOPAP. We have divided this task into the following areas, which are described separately below: 1) retroreflector-array transfer functions, 2) systems analysis — simulation, and 3) systems analysis — instrumentation. This division was made to represent a balanced effort among understanding the capability of currently available systems, exploiting this capability to the fullest extent, and developing new systems and subsystems.

3.8.1 Retroreflector-array transfer functions

The analysis for the retroreflector-array transfer function for NTS-1 has been published and distributed. The transfer function for Starlette has been completed, and a report is in press. The analysis on Starlette has already been used to compute camera and laser visibilities; a draft of the final report detailing the techniques used in the analysis is now being reviewed.

3.8.2 Systems analysis — Simulation

Support was provided to the Analytical Satellite Geophysics Department in the development and application of systems simulation software.

3.8.3 Systems analysis — Instrumentation

Analysis on the laser wavefront-distortion experiments has been completed; this work was carried out by Lehr and Pearlman of SAO and Billiris and Dr. M. D. Papagiannis of Boston University. Billiris presented the results as a Master's thesis to Boston University. The team found that the random error in measuring a fixed distance was reduced to the theoretical minimum set by quantal noise. With the random error minimized, wavefront distortion was measured; the results shown in Table 10. They drew the following conclusions about wavefront distortion:

Table 10. Wavefront distortion.

Experiment	Wavefront distortion probability of existence (%)	rms value (nsec)
1	100.0	0.3
2	100.0	0.4
3	100.0	0.6
4	59.4	0.5
5	94.8	0.6
6	72.6	0.6

A. Wavefront distortion does exist and may introduce range errors of a meter or more.

B. The distortion pattern changes with time and cannot be predicted.

C. Range errors introduced by the distortion are systematic and cannot be extracted from range data alone.

D. Range-error variations occur over such a small scale that they cannot be adequately calibrated out.

The effect of water-vapor absorption on return signal strength was investigated extensively for all four observing stations, with tests performed under a variety of atmospheric conditions. It was thought that atmospheric water vapor might be partially responsible for the 6- to 10-db signal loss, which cannot be accounted for by the present form of the range equation. Experimental results indicate, however, that the loss is too large to be due to water-vapor absorption. This conclusion is based on work done at the University of Texas (Johnson, 1972).

3.8.4 Evaluation of the new pulse processor

Analysis of data from the newly installed pulse-processing system is carried out with support from both OTDA and OA. The results of these analyses are reported in Section 2.4.

3.9 Orbit-Computation Techniques (RTOP 161-05-05)

Present analytical solutions for satellite motion are being improved by developing higher order perturbation terms, largely through the use of literal computer algebra. Semianalytical and numerical techniques are needed for refining the nongravitational effects in our orbit-computation routines. All theoretical developments are being verified by comparison with numerical integration and actual observations. These and other aspects of our orbit-computation program are described more fully in the following subsections. The objective of these studies is to develop an algorithm of 1-cm accuracy for computing satellite ephemerides. Simultaneously, we are developing minicompu-

ter software for computing real-time laser pointing angles, for determining orbital elements, and for processing data in the field.

3.9.1 Computer algebra

Dr. H. Kinoshita has added functions treating integration, differentiation, and numerical evaluation of finite trigonometric series to the computer's manipulation system.

3.9.2 Gravitational perturbations

The longitude-dependent part of the geopotential usually gives rise only to short-period effects in the motion of an artificial satellite. However, when the motion of a satellite is commensurable with that of the earth, the path of the satellite repeats itself relative to the earth and perturbations build up at each passage of the satellite in the same spot, so that there can be important long-period effects.

In order to take these effects into account in deriving a theoretical solution to the equations of motion of an artificial satellite, it is necessary to select terms in the longitude-dependent part of the geopotential that will contribute significantly to the perturbations. Ms. B. Romanowicz has been attempting to make a selection that is valid in a general case, regardless of the initial eccentricity of the orbit and of the order of the resonance.

Romanowicz has worked out a formal expression for solving the artificial-satellite theory by using Hori's method by Lie series, including resonant terms in the tesseral harmonics. Formal calculations have been made to incorporate long-period terms, and the formal solution is being compared to numerical integration. Romanowicz is preparing an SAO Special Report on this problem (Romanowicz, 1975).

In assisting Romanowicz with her resonance theory, Dr. K. Aksnes found that more terms should be included in the perturbation expressions. These

terms are now being derived, and it is hoped that improved agreement with numerical integration will result.

3.9.3 Radiation-pressure perturbations

Aksnes' semianalytical theory for computing the perturbations of earth satellites due to direct solar radiation pressure has been documented and submitted to Celestial Mechanics. He also presented a paper on this subject at the annual meeting of the American Astronomical Society (AAS) Division on Dynamical Astronomy in Tampa, Florida, in December (Aksnes, 1974).

Aksnes' algorithm has been tested through numerical integration of the equations of motion and through comparisons with observations of the balloon satellite 1963 30D during a 200-day interval. The results, which are in fairly good agreement with an orbit analysis recently published by Slowey (1974), are being incorporated into Aksnes' documentation. The evolution of the perturbations from the theory, the integration, and the observations agrees internally to 1% or better, with the exception of the perturbations in the semimajor axis, δa. When the paper was first being prepared, no satisfactory explanation was found for a much larger discrepancy of about 10% between the three different evaluations of δa. Subsequently, while performing similar tests for the balloon satellite Pageos, the source of this enigmatic discrepancy was traced to an inaccurate computation of the boundaries (E_1 and E_2) of the earth's shadow. During one revolution of this satellite, δa exhibits a short-period oscillation of about 600 m; however, during a 120-day period, the net variation of δa is on the average only roughly 10 m rev^{-1}. Such near cancellation of the short-period terms does not occur in the other five elements. Hence, in order to maintain the same degree of accuracy in δa as in the other elements, E_1 and E_2 need to be computed more accurately than the ±2° tolerance used in the theory. Furthermore, the integration, which was previously done with a fixed step size of about 3° in the mean anomaly, may also be expected to suffer a similar, though smaller, falloff in δa. By reducing the tolerance in the theory to ±0°.3 and by using a variable step size in the integration, an internal agreement of about 2% in δa results.

In the future, a more accurate and more efficient evaluation of E_1 and E_2, in which the earth's oblateness will also be taken into account, will be developed on the basis of a formulation due to Slowey.

Aksnes has also generated some test runs on Lageos, Starlette, and Geos 1 to find out how these satellites are affected by direct radiation pressure. These test cases will be included in the final documentation.

The comparison between theory and observations of the radiation-pressure perturbations affecting satellite 1963 30D has been extended to include the effect of the earth's albedo radiation. Although the albedo perturbations amount to only a few percent of the direct effect for this satellite, their inclusion improves the agreement with the observations during the 200-day interval considered.

The second approximation to the earth-albedo perturbations has been incorporated into the precision orbit-computation program and is apparently working. In this theory, the albedo of the earth is uniform and there are no restrictions on the eccentricity or inclination of the satellite orbit or on the position of the sun. The next approximation, which includes a better model for the force when the satellite is in the vicinity of the terminator, has been completed and is ready for programing. Dr. D. A. Lautman (1974) presented a documentation of his complete albedo-perturbation theory for the case of a uniform albedo at the AAS meeting in December.

Lautman has begun improving his perturbation theory for close-earth satellites due to radiation diffusely reflected from the earth, in which the earth's albedo has a latitudinal dependence given by $A = A_0 + A_2 \sin^2 \phi$. Two difficulties have been overcome: the first due to an unacceptably slow convergence of the trigonometric series used to express the force, and the second due to a singularity in the series for a particular sun-orbit orientation.

While a uniform albedo can be fitted to the Tiros albedo data with a relative error of about 25%, the form $A = A_0 + A_2 \sin^2 \phi$ can be fitted with a

relative error of about 8%. Owing to the small magnitude of the albedo perturbations, it is felt that any further complexity in the albedo model is not warranted.

The theory for a latitudinal variation in the albedo is far more complicated than the one for a uniform albedo. For example, while the expressions for the three components of the disturbing acceleration in the nonterminator case for a uniform albedo contain seven terms, each of which can be expanded into a terminating Fourier series, the present theory requires about 70 terms for the same case, many of which cannot be expanded in finite form. A number of terms have $\csc^2 \psi$ as a factor, where ψ is the geocentric angle between the sun and the satellite. By writing

$$\csc^2 \psi = \frac{1}{1 - C^2 \cos^2 (u - \phi)} \quad ,$$

where $C \cos (u - \phi) = \cos \psi$ and u is the argument of the latitude, an expansion can be found of the form

$$\csc^2 \psi = \frac{2}{\sqrt{1 - C^2}} \left[\frac{1}{2} + \sum_{n=1}^{\infty} K^n \cos 2n(u - \phi) \right] \quad ,$$

where

$$K = \frac{1 - \sqrt{1 - C^2}}{1 + \sqrt{1 - C^2}} \quad \text{and} \quad C < 1 \quad .$$

The expansion in terms of K converges much more rapidly than one in terms of C, since K is less than C. The above series diverges if $C = 1$ (i.e., if the sun is in the orbital plane), but the factors of $\csc^2 \psi$ combine in such a way that the coefficient of each periodic term is of the form

$$\frac{\text{const}}{\sqrt{1 - C^2}} (K^n - K^{n+m}) \quad ,$$

which can be written

$$\text{const} \times K^n(1 + K) \sum_{j=0}^{m-1} K^j \quad .$$

The above expression remains finite at C = K = 1, and the series maintains its form through the singularity.

3.9.4 Lunar-solar tidal perturbations

A method for calculating tracking-station displacements resulting from lunar and solar body tides has been determined by Williamson and Gaposchkin. Because body-tide displacements can be as large as 36 cm, it is important to account for them if orbits with 1-cm accuracy are to be obtained. The displacements are being incorporated in a special version of the department's precision orbit-computation program. One of the modifications to the program is a subroutine to account for the interaction of J_2 terms with some of the long-period perturbations.

The effects due to the motion of the equatorial plane on the orbital elements of an artificial satellite, which had been neglected in a previous theory by Kozai and Kinoshita (1973), have now been calculated and incorporated in the precision orbit-computation program. The theory adopts the International Astronomical Union's (IAU) precession constants derived from the rigid earth. Effects on inclination due to the difference between the nutational constants derived from a rigid earth (IAU) and those from a nonrigid earth (Jeffreys and Vicente, 1957a,b; Kakuta, 1970) have been calculated. They are of the same order as the effects from the nutational terms neglected by Kozai and Kinoshita (1973). These effects have been calculated for Geos 1.

3.9.5 Reference systems

Literal expressions for the precessional motion of the mean equator referred to an arbitrary epoch have been completed (Kinoshita, 1975). Their numerical representations are based on values recommended at the working meeting of the IAU Commission No. 5 held in Washington, D.C., in September. In

constructing the equations of motion, the second-order secular perturbation and the secular perturbation due to long-period terms in the motions of the moon and the sun have been considered. These perturbations contribute more to the motion of the mean equator than does the term due to the secular perturbation of the orbital eccentricity of the sun. The correction $\Delta f = 1''.10$ (Fricke, 1971) to Newcomb's lunisolar precession, the correction $\Delta g = -0''.03$ (Laubscher, 1972) to Newcomb's planetary precession, and the geodesic precession $f_g = 1''.915$ (de Sitter, 1938) are all used.

Kinoshita's new theory for the nutation of three planes (the plane normal to the angular-momentum axis, the equatorial plane, and the plane normal to the rotational axis) and their numerical representations have been completed. Woolard's (1953) theory includes some secular terms that have an important effect on the establishment of a reference system but whose existence cannot be believed from the standpoint of conservative mechanics. The present theory does not include such secular terms.

If the mass ratio between the moon and the earth is assumed to be given, instead of a nutational constant, then the nutational constant and the dynamical ellipticity of the earth can be determined theoretically. Adopting the values $M_\oplus/M_\mathbb{C} = 81.3007$ (Jet Propulsion Laboratory (JPL)), geodetic precession $= 1''.915$ per tropical century (de Sitter, 1938), and proper motion $= 1''.1$ per tropical century (Fricke, 1971), and applying to his rigid theory the nonrigid earth models of Jeffreys and Vicente (1957a,b), Pederson (1967), Molodensky (1961), and Kakuta (1970), Kinoshita has derived theoretical coefficients of the main nutational terms, shown in Table 11. The results of this work are being written up and will be submitted to Celestial Mechanics (Kinoshita, 1974).

3.9.6 Numerical integration

With an objective of determining satellite ephemerides of 1-cm accuracy over 2-week periods, the numerical-integration program will be used as a tool for verifying all analytical theories.

Table 11. Nutation coefficients for the axis of the figure of a nonrigid earth.

Model	Ω		$2L_{\odot}$		$2L_{\varsigma}$	
	$\Delta\varepsilon$	$-\sin\varepsilon\,\Delta\psi$	$\Delta\varepsilon$	$-\sin\varepsilon\,\Delta\psi$	$\Delta\varepsilon$	$-\sin\varepsilon\,\Delta\psi$
Rigid	9.2269	6.8710	0.5537	0.5084	0.0950	0.0882
Jeffreys-Vicente (1957a)	9.2022	6.8378	0.5743	0.5250	0.0977	0.0904
Jeffreys-Vicente (1957b)	9.2194	6.8607	0.5414	0.4896	0.0977	0.0904
Pederson (1967)	9.2023	6.8393	0.5737	0.5244	0.0979	0.0906
Molodensky (1961)	9.2000	6.8363	0.5748	0.5255	0.0977	0.0903
Molodensky (1961)	9.2034	6.8407	0.5672	0.5183	0.0973	0.0900
Kakuta (1970)	9.1815	6.8134	0.5811	0.5319	0.1008	0.0935

The forces modeled in the numerical-integration program are the earth's gravitational force, lunar and solar direct-gravitational and body-tide forces, direct solar-radiation pressure, and earthshine radiation pressure. The program uses a general-purpose Adams-type integrator supplied to us by F. Krogh at JPL. Williamson and Gaposchkin have completed checking the program, and an internal report describing the forces modeled and the use of the program has been prepared.

Because the error estimate of the Adams integrator is not reliable for our problem, we are continuing to study alternate integration techniques.

3.9.7 Field computing capability

The stand-alone mode for the field minicomputer systems provides stations with the means for computing look angles from orbital elements and therefore should reduce the communications volume now required to send predictions to stations. Incorporated in the system are a prediction loop and facilities for avoiding the sun and zenith. Features have been added to the input massager to allow transmission of gravity fields. The paper-tape output program has been written and debugged; it offers four choices of punch and output code. Forecast and pass summary reports have been written and debugged. Programs have been added to the software to compute the estimated signal strength returned from a satellite. The power-failure recovery routine has been implemented in the Forth language and seems to be working. Linc-tape diagnostics have been improved.

Some other improvements that have been made to the stand-alone programing system follow:

A. It is now no longer possible for an operator to type an invalid command and wipe out the system. Invalid commands are flagged with proper diagnostics.

B. Decimal points are no longer mandatory in typed numbers.

C. A new program identifies periods when no return is expected from a satellite.

D. The basic prediction process has been speeded up by 30%.

E. Another program checks to see that the tesseral harmonics have been recently updated.

Other programs written for this system include one to copy Forth code to seven-track magnetic tape for the Nova and another to convert ASCII files from magnetic tape to BCD for listing or input to other programs on the CDC 6400.

The departmental minicomputer has a full complement of peripherals similar to the field units, in order to facilitate future development and maintenance of field systems. In addition, an industry-compatible magnetic-tape unit has been attached to allow for easy transfer of large numbers of data at high or low densities between the minicomputer and the CDC 6400. A dual-drive disk storage system has also been attached; it provides about 5 million 16-bit words of mass storage, with an average access time approximately two orders of magnitude less than previously available.

3.10 Solid-Earth Surface Measurements (RTOP 161-05-06)

Mohr's (1974a) Special Report on major structures of the African rift system was published in October.

The fifth expedition to resurvey the Ethiopian Rift, funded by the Smithsonian Research Foundation, was successfully concluded in December. Beforehand, various network configurations were analyzed to establish where new lines should be added to decrease the limit of detection of station motions. Since previous analysis of the Adama network indicated crustal extension at a rate of approximately 1 cm $year^{-1}$, emphasis during this resurvey was placed on measurements of this network (Figure 8).

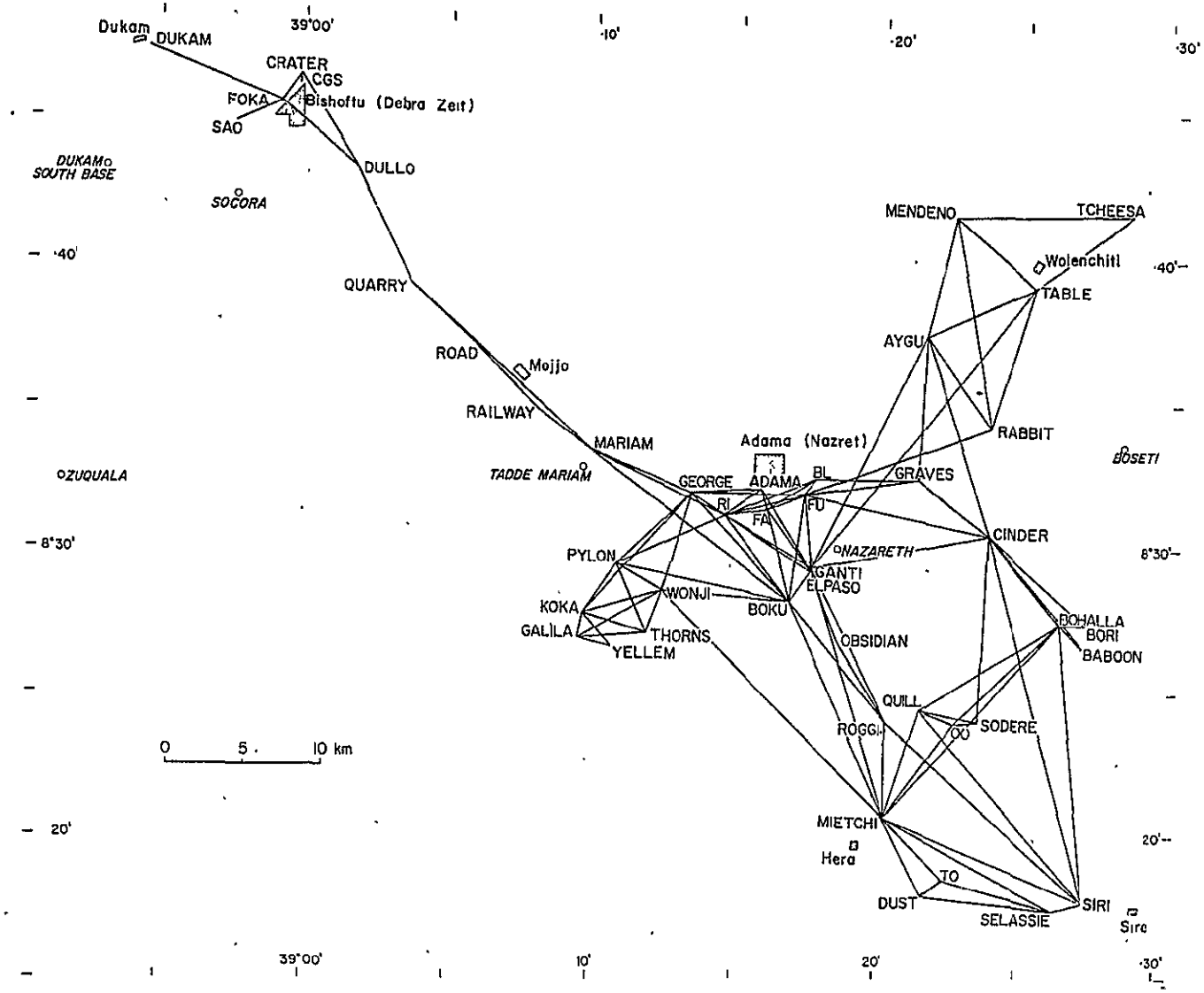

Figure 8. The northern (Adama) geodimeter network, Ethiopian rift valley, after the 1974 survey.

In addition, the central rift network was remeasured and extended (Figure 9), and two new networks in east-central Afar were established (Figure 10). These new networks overlay a zone of crustal deformation that extends inland from the Gulf of Aden spreading zone. Mohr, who led the expedition, anticipates that crustal extension in this area will be 1 to 2 cm $year^{-1}$, as opposed to the 1 cm $year^{-1}$ or less found in the rift valley.

A total of 514 lines was measured with the SAO geodimeter. A computer program has been modified to accept data from the latest resurvey, and additional information on distances, azimuths, and heights of auxiliary points from the main stations has been obtained.

A program has also been written, by Girnius, to compute error ellipses and standard-error curves.

Tentative geodimeter station-displacement vectors resulting from least-squares adjustment of the Wolenchiti, the Langana, and part of the Adama geodetic networks for the period 1969 to 1973 have been summarized in a paper presented at the International Symposium on Recent Crustal Movements in August in Zurich, Switzerland (Mohr, Girnius, Cherniack, Gaposchkin, and Latimer, 1974). Although the period of observations in the Ethiopian rift is rather short for firm conclusions to be drawn, it is clear that some real tectonic movements have been detected.

Mohr and Girnius have begun to reduce the data and analyze them within the context of previous Ethiopian surveys. The knowledge gained from this study of crustal deformation will supplement our precision satellite-tracking techniques of measuring plate motion and deformation.

In order to test the long-term stability of the geodimeter being used, a continually monitored baseline has been established along the Charles River in Cambridge. The base consists of two lines, 44 and 75 m long, with three brass plugs set into concrete pads. The lines have been measured with both steel tape and the geodimeter. Other lines had been considered, and recommendations were received from a local geodetic agency.

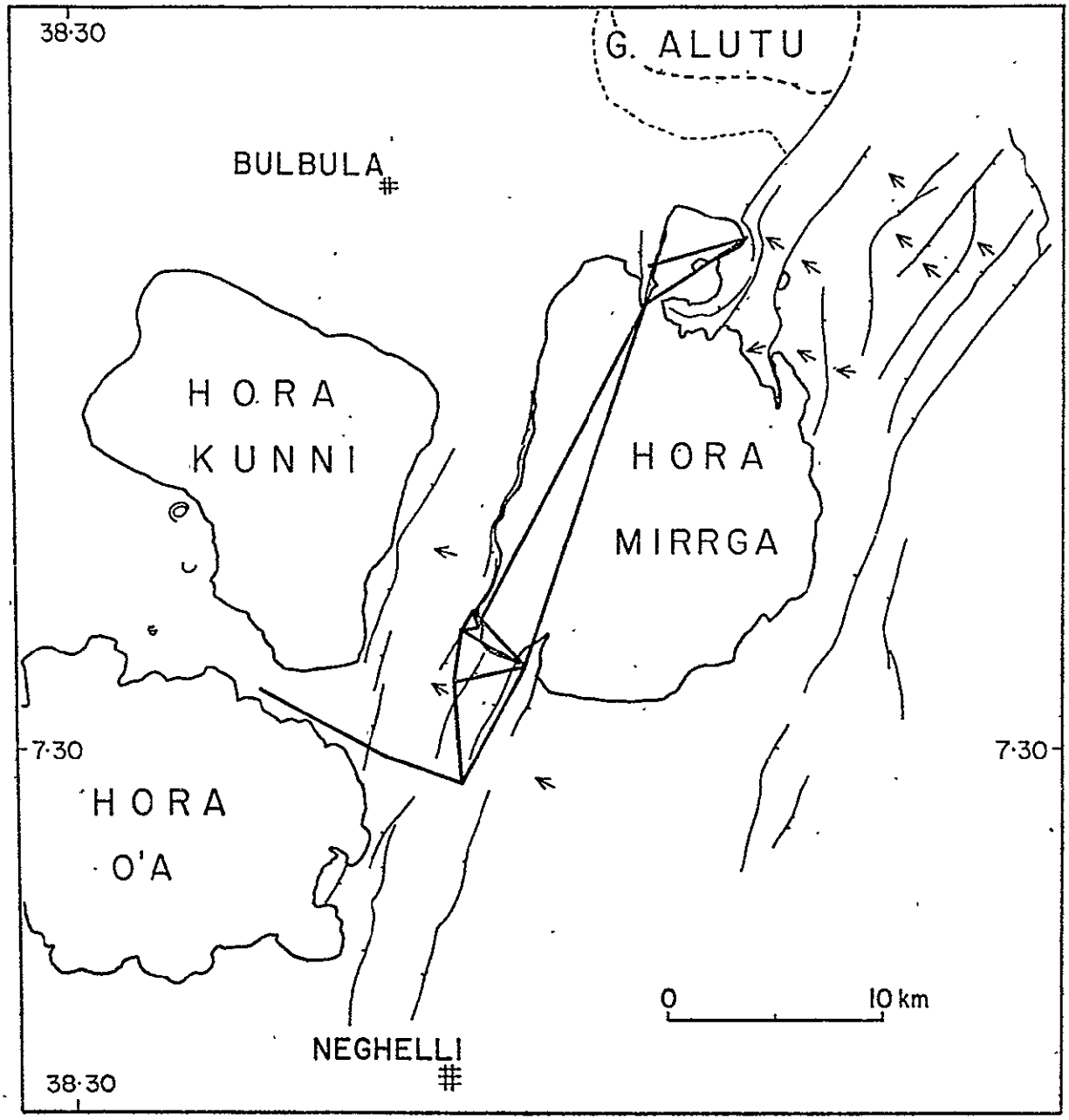

Figure 9. The central (Mirrga) geodimeter network, Ethiopian rift valley, after the 1974 survey. Not all the lines in the southern part of the network can be shown at this scale.

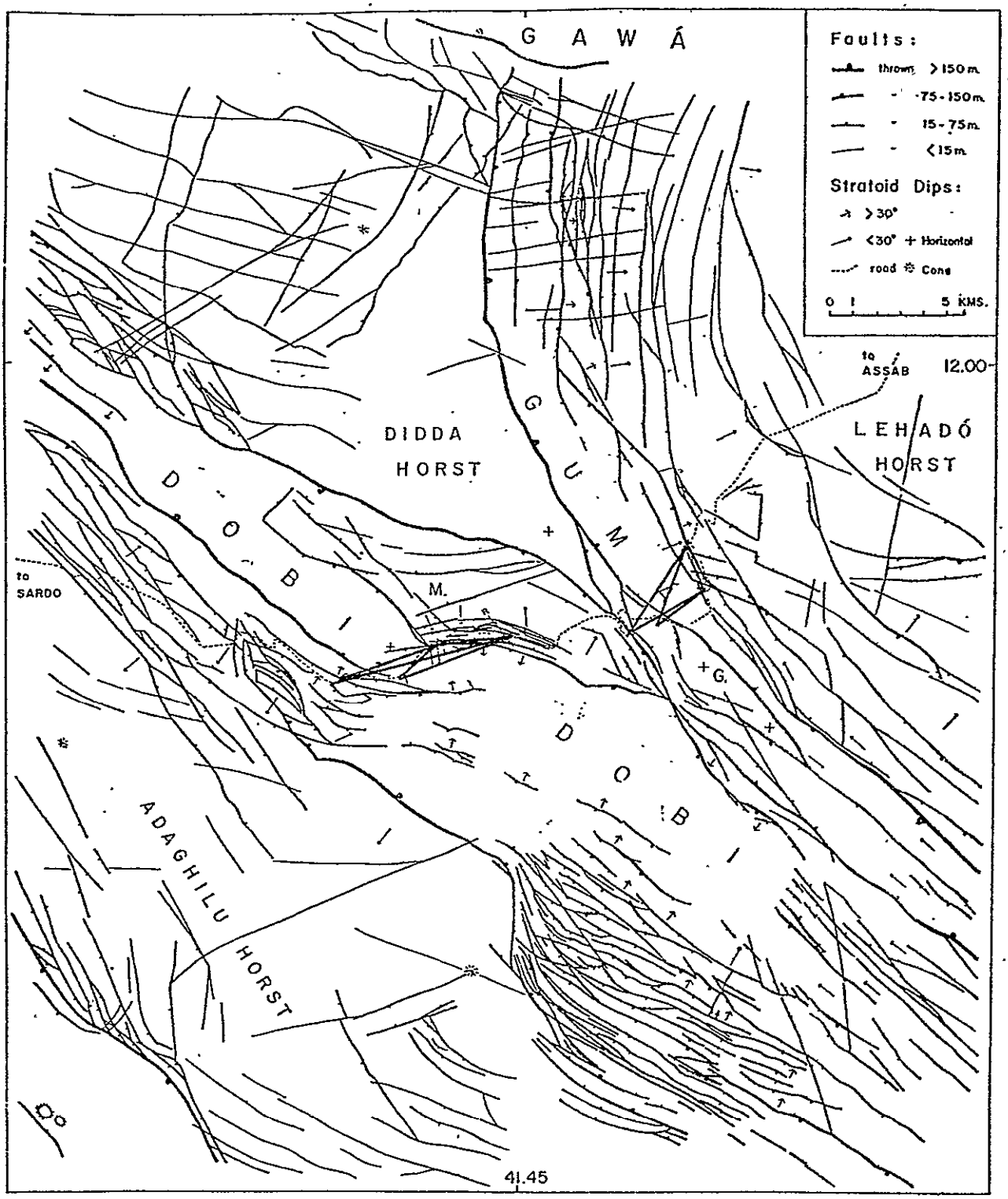

Figure 10. The two quadrilaterals established in central Afar in 1974, crossing, respectively, the Dobi and Guma gräben.

Mohr (1974b) also discussed atmospheric-correction problems pertaining to geodimeter surveys at a meeting of the International Association of Geodesy in Stockholm, also in August. Dealing largely with financial, logistic, and instrumental realities, this topic received much useful comment for future resurveys in Ethiopia, and lively discussions were had with survey leaders from other parts of the world.

Mohr then traveled to Lidingö to confer with AGA on the operation and maintenance of the SAO Mk 8 geodimeter. Since then, he has checked out the new laser unit and readjusted the optical alignment in this geodimeter.

Also during this period, Mohr discussed rift-valley geophysics with Dr. R. W. Girdler at the University of Newcastle, rift geochronology and geochemistry with scientists at the University of Leeds and the University of Leicester, and rift geochronology with staff members at the National University in Addis Ababa.

While abroad, Mohr was able to devote some time to the collection of manganiferous rock speciments from Y Llethr, Moelfre, and Rhinog Fach in North Wales; he has been studying their significance to the opening of the Atlantic Ocean in the early Paleozoic.

4. ATMOSPHERIC RESEARCH

Work in this area has proceeded along several lines, discussed in the following subsections. Routine determinations of total density from the drag on several satellites have continued, plus special studies on selected satellites to test results from *in situ* experiments. About half the ion-current intensities from ESRO 4 have been reduced to number densities, and the extensive analysis of these data has begun. Meanwhile, basic revisions have been made to models of temporal variations; the models are now in general agreement with satellite-drag and mass-spectrometer data.

4.1 Density Determinations

Some special work is in progress on the determination of atmospheric densities from satellite drag in collaboration with Prof. M. Römer of the Astronomische Institute in Bonn. Römer came to SAO in December to discuss these analyses. The satellites involved are 1972 92A (ESRO 4), 1972 100A (AEROS 1), and 1974 55A (AEROS 2). The drag densities from these satellites are of particular interest as they will provide a test of results from *in situ* experiments on the satellites. The data in hand indicate generally good agreement between the total density determined by the mass spectrometer on ESRO 4 and that in the 1972 COSPAR International Reference Atmosphere model. There are, however, small systematic differences, just as there are when densities from drag are compared with any of the available models. A much more conclusive comparison may be possible by using the results of direct drag analysis.

We have also continued with the routine determination of total density from the drag on a number of satellites. Some of these densities, which may span 15 years or more, are being utilized in the study of superrotation (Section 4.4). Drag densities from Explorer 32 and OV3-3 are also being compared with the total density inferred from the ESRO 4 mass spectrometer to test the validity of the ESRO 4 results.

Six satellites are being used in this program: 1959 α1 (Vanguard 2), 1960 ξ1 (Explorer 8), 1963 53A (Explorer 19), 1966 44A (Explorer 32), 1966 70A (OV3-3),

and 1968 66A (Explorer 39). The effective height at which densities are obtained ranges from 300 to 800 km, and the inclinations extend from 33° to 81°, allowing almost complete global coverage. Use is made of Baker-Nunn photographic positions and of radar data supplied by the U.S. Air Force Command. All the steps in the work (orbit computations, fitting of elements, computation and graphing of residuals from fitted elements, and finally, computation of atmospheric densities) have been completed through July 1974, and the new data have been added to the corpus of uninterrupted density data, now numbering about 50,000 and extending back to 1958. Either directly, or indirectly through models based on them, these densities are used all over the world for comparison with instrument measurements.

4.2 Analysis of ESRO 4 Data

Slowey spent nearly 3 months at the Physikalisches Institut of the University of Bonn working with Prof. U. von Zahn on the development of software for the reduction of data from the gas analyzer on the ESRO 4 satellite. More than 1 million ion-current intensities were reduced to number densities, and Slowey returned to SAO in November with tapes containing all the number densities of four atmospheric species (N_2, O, Ar, and He) at heights below 350 km for most of the first 260 days of the active lifetime of the satellite. The measurements extend from December 1972 to August 1973. It is expected that Slowey's programs will be used to generate number densities for the remaining 240 days of the satellite's lifetime as the additional ion currents are reduced from the telemetry data; these data will be received in Cambridge during the next few months. Much of the laborious work of converting these nine-track IBM tapes to a format usable on SAO's computer is being done by Mr. I. G. Campbell.

Jacchia and Slowey have begun to analyze the data; they are optimistic that such a profusion of information will enable substantial improvements to be made to current atmospheric models.

While waiting for the computer programs to be prepared, Jacchia began a preliminary analysis by hand of some of the data at 280 km listed in printout Slowey made in Bonn. This computer printout gives approximately 5000 sets of number densities

for the two points on each orbit where the satellite height was as close to 280 km as possible. Selecting data from quiet and disturbed days, Jacchia tested an approximate formula, derived from published OGO 6 data, for changes in composition with geomagnetic activity and location. With a change in one of the constants, the formula approximates the ESRO 4 data over a wide range of geomagnetic activity. This formula will be a guideline for future analyses, and the residuals will be used to gain further insight into the global mechanism of atmospheric perturbations.

A study of the perturbed periods 31 March to 3 April and 12 to 16 April 1973 clearly shows that the character of the atmospheric perturbation at low latitudes is radically different from that at high latitudes. In the equatorial region, all four recorded atmospheric species vary in phase by approximately the same amount, with a lag of about 8 hours with respect to the planetary index K_p. At high latitudes, by contrast, Ar varies in phase with N_2 with an amplitude of twice that of the latter, O shows very little variation, and the variations of He are an almost exact mirror image of those of N_2, with the maximum of the one corresponding to the minimum of the other. The behavior at high latitudes can be explained by assuming that temperature changes caused by the magnetic perturbations are accompanied by proportional changes in the height of the homopause. Such a change in the height of the homopause has been recently used to account successfully for smaller scale disturbances in composition (Blum, Wulf-Mathies, and Trinks, 1975). According to Jacchia's models, the mean molecular mass of the air at the effective homopause is 28.4. If it is made exactly 28 — i.e., the mass of nitrogen — we can write

$$\frac{\Delta \log n_i}{\Delta \log n(N_2)} = \left[\frac{\partial \log n_i/\partial T}{\partial \log n(N_2)/\partial T}\right]_T + \frac{[\partial \log n(N_2)/\partial z - \partial \log n_i/\partial z]_{z_H+}}{[\partial \log n(N_2)/\partial T]_T} \frac{dz_H}{dT}$$

$$= A_i + B_i \frac{dz_H}{dT} \quad ,$$

where n_i is the number density of species i, T is the temperature, and z_H is the height of the homopause. At 280 km, the coefficients on the right-hand side

are nearly constant for each species. Taking $dz_H/dT = 30$ m $°K^{-1}$ and evaluating A_i and B_i from his models, Jacchia has found the following factors for $\Delta \log n_i/\Delta \log n(N_2)$: Ar = 1.92, N_2 = 1.00, O = -0.10, and He = -0.83. With these values, the variations of Ar, O, and He can be derived from those of N_2 with spectacular accuracy, one almost comparable to the observational error.

At low latitudes, as we said, the variations are well correlated with the planetary geomagnetic index K_p, with a time lag of about 8 hours. At high latitudes, however, there is no time lag with respect to the magnetic perturbation, and details of the variation indicate a possible correlation with the auroral electrojet index AE — which, unfortunately, is not yet available for 1973. Dr. J. H. Allen of the World Data Center in Boulder is trying to obtain some of the unpublished material for us. A preliminary global model of the variations using the K_p index has been developed, however.

Computer programs for use in the analysis of the ESRO 4 data are in preparation. A number of individual storm periods will be looked at before Jacchia and Slowey go on to a general solution for the variations associated with geomagnetic disturbances. Of particular interest at the moment is the detailed behavior in the transition region between high and low latitudes. A computer program to select data at different heights and to compute the effects of the other, quiet, variations will be completed in the near future. Then the disturbed variations can be studied in greater detail with respect to latitude and with considerably more ease.

4.3 Atmospheric Models

To lead the way for the analysis of ESRO 4 data, Jacchia started investigating the scant information available from OGO 6 on changes of composition in the disturbed thermosphere. The global picture of the disturbed thermosphere is very complex: heating in the auroral zone distorts the temperature profiles of the static models; winds and gravity waves propagate to lower geomagnetic latitudes, where density variations are observed without important temperature changes; and, finally, the atmospheric constituents diffuse separately. Although Mayr and Volland (1973) attempted a dynamical theory of the disturbed thermosphere, it proved very

difficult to apply it to the construction of practical models. Consequently, Jacchia tried interpreting OGO 6 data by using correction terms in his static models. Good results were obtained by splitting the change in the number density of the atmospheric species into two terms, one purely thermal and the other a blanket term designed to take care of all the effects that are not accounted for by a simple increase of the exospheric temperature. The equations

$$\Delta T = [10\ K_p + 0.01 \exp(K_p)]\ (1 + 5 \sin^4 \phi_G)$$

$$\Delta \log_{10} n_i = 0.0012 \Delta T_0 \left[1 + 5\left(\frac{M_i}{28} - 1\right) \sin^4 \phi_G\right],$$

used with a time lag dependent on ϕ_G, seem to represent the data to a first approximation. Here ΔT is the increase in exospheric temperature corresponding to a change in the geomagnetic index K_p from zero to its proper value (ΔT_0 is the equatorial value of ΔT), ϕ_G is the geomagnetic latitude, n_i is the number density of species i, and M_i is its molecular mass.

Jacchia has also continued improving analytical expressions for other types of atmospheric variation. More recent mass-spectrometer data from ESRO 4 plus those from OGO 6 have shown that changes of composition not accounted for by previous models accompany every change in atmospheric temperature and density. This fact has necessitated a thorough revision of the models of the temporal variations. In the course of this revision, even the basic relations, such as that between temperature and solar activity (tied to the 10.7-cm flux), have been overhauled. Previous attempts at modeling the diurnal variation on a global basis had led to an unsatisfactory result, namely, a dependence on height of the latitude at which the maximum global temperature occurs at the time of solstices. If true, this would have violated the isothermal character of the atmosphere above the thermopause. It has now been found that by keeping the intrinsic seasonal-latitudinal variations of the atmospheric species constant throughout the atmosphere — such as would occur if they were caused by a change in height of the homopause — we can keep the latitude of the maximum temperature at the time of solstices independent of height. An oscillation of 12 km in the height of the thermopause around its mean value accounts for the observed variations in Ar, N_2, O and He and eliminates the

difficulties previously encountered with the diurnal variation. Further analysis of the ESRO 4 mass-spectrometer data should, of course, improve the models even more.

Also, the variation in hydrogen concentration with solar activity has been reanalyzed on the basis of new data and fitted with a simpler equation, more in line with the physics of escape. The models are now in broad agreement not only with satellite-drag and mass-spectrometer data, but also with temperatures determined from doppler broadening of the 6300 Å line and from incoherent scatter of radio waves.

4.4 Atmospheric Rotation

Slowey has completed his work on systematic winds in the earth's atmosphere as determined from the decrease in orbital inclination of four balloon satellites during decay. A paper describing these winds at heights between 350 and 375 km has been accepted for publication (Slowey, 1975).

Since his return from Germany, Slowey has been continuing his analysis of the orbital inclinations of satellites to determine mean rates of rotation of the earth's upper atmosphere — the so-called "superrotation" rate. Five satellites, with heights ranging from 250 to 200 km, are currently being studied. The results obtained at greater heights will either confirm or deny his earlier finding, inferred from the balloon satellites, that a net superrotation persists to well over 350 km. The results at lower heights will also be interesting, as the amount of the superrotation may well be considerably less than is now generally accepted.

The set of zonal-harmonics coefficients from the 1973 Smithsonian Standard Earth (III), truncated at the 23rd order, has been incorporated into the precise orbit-computation program for use in the study of atmospheric rotation.

4.5 Search for Lunar Tides

Long series of densities derived from satellite drag were analyzed in the hope of finding evidence of lunar tides in the thermosphere and exosphere. Preliminary results showed a diurnal oscillation in phase or antiphase with local lunar time with an amplitude of 3 to 5% in density. The analysis was based on the assumption that the atmosphere's tidal response would not be greatly different from the tidal-force input, as, for example, is true for midoceanic tides. This assumption was applied to 15 sets of observations, with the expectation that the resulting phase shifts and amplitudes would undergo some consistent variation with perigee height — or with mean density at perigee height. The analysis was refined by introducing the declination and distance of the moon.

Subsequent investigations, however, did not bear out the preliminary findings. What were taken to be real tidal effects were, in fact, spurious contributions from systematic modeling errors, caused by the impossibility of rigorously accounting for the "27-day" variation connected with solar rotation. The presence of this 27-day variation makes it all but impossible to detect atmospheric lunar tides from satellite drag. It was already known that the solar component is completely overwhelmed by the daily density variations of thermal origin. Since the connection of lunar tides with the 27-day solar variation is not so obvious, the negative results of the search have been briefly summarized for publication in the Journal of Geophysical Research (Jacchia, 1975).

4.6 Other Activities

The Committee for the Extension of the U.S. Standard Atmosphere held its final meeting in Washington, D. C., in November. Jacchia has been the Working Group Chairman for 15 years, as well as the convener for the task group concerned with data above 200 km. The manuscript for the new Standard Atmosphere, which Jacchia helped coordinate and write, is essentially complete and will be published in 1975.

5. REFERENCES

AKSNES, K.

1974. Short-period and long-period perturbations of a spherical satellite due to direct solar radiation. Presented at the Dynamical Astronomy Division Meeting of the American Astronomical Society, Tampa, Florida, December; submitted to Celest. Mech.

BLUM, P.W., WULF-MATHIES, C., and TRINKS, H.

1975. Interpretation of local thermospheric disturbances of composition observed by ESRO 4 in the polar region. In Space Research XV, in press.

DE SITTER, W.

1938. On the system of astronomical constants. Bull. Astron. Inst. Netherlands, vol. 8, pp. 213-216.

FRICKE, W.

1971. Determinations of precession. Celest. Mech., vol. 4, pp. 150-162.

GAPOSCHKIN, E. M.

1973a. 1973 Smithsonian Standard Earth (III) (editor). Smithsonian Astrophys. Obs. Spec. Rep. No. 353, November, 388 pp.

1973b. Investigations of earth dynamics from satellite observations. Final Report, NASA Grant NGR 09-015-103, March.

1974. Earth's gravity field to the eighteenth degree and geocentric coordinates for 104 stations from satellite and terrestrial data. Journ. Geophys. Res., vol. 79, pp. 5377-5411.

1975. Quadrennial report to the International Union of Geodesy and Geophysics — Dynamic satellite geodesy (1971-1975). Trans. Amer. Geophys. Union, in press.

GAPOSCHKIN, E. M., LATIMER, J., and MENDES, G.

1974. Station coordinates in the Standard Earth III system derived by using camera data from ISAGEX. Presented at the INTERCOSMOS Symposium on Results of Satellite Observations, Budapest, October.

JACCHIA, L.G.

1975. A search for lunar tides in the thermosphere. Journ. Geophys. Res., in press.

JEFFREYS, H., and VINCENTE, R. O.

1957a. The theory of nutation and the variation of latitude. Mon. Not. Roy. Astron. Soc., vol. 117, pp. 142-161.

1957b. The theory of nutation and the variation of latitude: The Roche model core. Mon. Not. Roy. Astron. Soc., vol. 117, pp. 162-173.

JOHNSON, M. M.

1972. Measurement of the spatial distribution of atmospheric water vapor using a ruby laser. Ph.D. Thesis, The University of Texas at Austin.

KAKUTA, C.

1970. The effect of a compressible core on Molodensky's theory of earth tides. Publ. Astron. Soc. Japan, vol. 22, pp. 199-222.

KAULA, W.M.

1967. Theory of statistical analysis of data distributed over a sphere. Rev. Geophys., vol. 5, pp. 38-107.

KINOSHITA, H.

1974. Theory of the rotation of the rigid earth. To be submitted to Celest. Mech.

1975. Formulas for precession. Smithsonian Astrophys. Obs. Spec. Rep., in press.

KOZAI, Y., and KINOSHITA, H.

1973. Effects of motion of the equatorial plane on the orbital elements of an earth satellite. Celest. Mech., vol. 7, pp. 356-366.

LAUBSCHER, R. E.

1972. A determination of the motion of the ecliptic. Astron. Astrophys., vol. 20, pp. 407-414.

LAUTMAN, D. A.

1974. Perturbations of a close earth satellite due to sunlight reflected from the earth. Presented at the Dynamical Astronomy Division Meeting of the American Astronomical Society, Tampa, Florida, December.

MAYR, H. G., and VOLLAND, H.

1973. Magnetic storm characteristics of the thermosphere. Journ. Geophys. Res., vol. 78, pp. 2251-2277.

MOHR, P. A.

1974a. Mapping of the major structures of the African Rift system. Smithsonian Astrophys. Obs. Spec. Rep. No. 361, October, 70 pp.

1974b. Atmospheric correction problems in Ethiopian geodimeter surveys. Presented at the International Association of Geodesy Meeting, Stockholm, August.

MOHR, P.A., GIRNIUS, A., CHERNIACK, J. R., GAPOSCHKIN, E. M., and LATIMER, J.

1974. Recent crustal deformation in the Ethiopian Rift valley. Presented at the International Symposium on Recent Crustal Movements, Zurich, August.

MOLODENSKY, M.S.

1961. The theory of nutation and diurnal earth. In Quatrième Symposium International sur les Marées Terrestres, Comm. Obs. Roy. Belgique No. 188, Ser. Geophys. No. 58, pp. 25-56.

PEDERSON, G. H.

1967. The effect of the fluid core on earth tides. M.Sc. Thesis, University of Waterloo, Ontario.

ROMANOWICZ, B. A.

1975. On the tesseral-harmonics resonance problem in artificial-satellite theory. Smithsonian Astrophys. Obs. Spec. Rep., in press.

SLOWEY, J. W.

1974. Radiation-pressure and air-drag effects on the orbit of the balloon satellite 1963 30D. Smithsonian Astrophys. Obs. Spec. Rep. No. 356, January, 93 pp.

1975. Systematic winds at heights between 350 and 675 km from analysis of the orbits of four balloon satellites. Planet. Space Sci., in press.

WILLIAMSON, M. R., and GAPOSCHKIN, E. M.

1975. The estimation of 550 km X 550 km mean gravity anomalies. Smithsonian Astrophys. Obs. Spec. Rep., in press.

WOOLARD, E. W.

1953. Theory of the rotation of the earth around its center of mass. Astron. Papers, vol. 15, part 1, 128 pp.